

Generating Quantum Matrix Geometry from Gauged Quantum Mechanics

Kazuki Hasebe

National Institute of Technology, Sendai College, Ayashi, Sendai, 989-3128, Japan

November 27, 2023

Abstract

Quantum matrix geometry is the underlying geometry of M(atrix) theory. Expanding upon the idea of level projection, we propose a quantum-oriented non-commutative scheme for generating the matrix geometry of the coset space G/H . We employ this novel scheme to unveil unexplored matrix geometries by utilizing gauged quantum mechanics on higher dimensional spheres. The resultant matrix geometries manifest as *pure* quantum Nambu geometries: Their non-commutative structures elude capture through the conventional commutator formalism of Lie algebra, necessitating the introduction of the quantum Nambu algebra. This matrix geometry embodies a one-dimension-lower quantum internal geometry featuring nested fuzzy structures. While the continuum limit of this quantum geometry is represented by overlapping classical manifolds, their fuzzification cannot reproduce the original quantum geometry. We demonstrate how these quantum Nambu geometries give rise to novel solutions in Yang-Mills matrix models, exhibiting distinct physical properties from the known fuzzy sphere solutions.

Contents

1	Introduction	3
2	Quantum-oriented non-commutative scheme	4
2.1	Behind the scene of the emergent matrix geometry	4
2.2	Non-commutative scheme for generating the matrix geometry	6
2.2.1	General prescription	7
2.2.2	Advantages	7
2.3	General Properties	8
2.3.1	Covariance	8
2.3.2	Beyond the commutator formalism	9
3	Matrix coordinates from the $SO(5)$ Landau model	10
3.1	The $SO(5)$ Landau model	10
3.2	Matrix coordinates	12
4	Pure quantum Nambu matrix geometry	15
4.1	The lowest Landau level matrix geometry	16
4.2	Higher Landau level matrix geometry	18
4.3	Nested fuzzy four-sphere	19
5	Internal matrix geometry	23
5.1	Fuzzy hyper-latitudes	23
5.2	Fuzzy three-sphere	24
6	Continuum limit and the S^4 geometry	26
6.1	The 2nd Hopf map	26
6.2	Continuum limit	27
6.3	S^4 geometry	28
6.3.1	Coherent state method	28
6.3.2	Probe brane method	29
7	Realization in Yang-Mills matrix models	30
7.1	Basic relations	30
7.2	As classical solutions of Yang-Mills matrix models	31
7.2.1	With a mass term	31
7.2.2	With a fifth-rank Chern-Simons term	33
8	Even higher dimensions	34
8.1	Landau level matrix geometries	34
8.2	Higher form gauge field and Yang-Mills matrix model	36
9	Summary and discussions	37
A	Groenewold-Moyal plane from planar Landau model	38
B	Two-sphere matrix coordinates in Yang-Mills matrix models	39
B.1	Basic properties	39
B.2	Matrix model analysis	41

1 Introduction

It has been almost eighty years since the inception of theoretical research on quantized space-time with Snyder's first explicit model [1, 2]. This research field continues to be active, contributing to a deeper understanding of space-time. Non-commutative geometry presents a promising mathematical framework for describing the microscopic nature of space-time [3]. A general mathematical framework of non-commutative geometry was set up by Connes [4]. More tangible non-commutative schemes are those such as deformation quantization, geometric quantization and Berezin-Toeplitz quantization [5]. As these ideas are rooted in the canonical quantization method of the phase space [6, 7], the corresponding non-commutative schemes are concerned with the quantization of the symplectic manifolds or Poisson manifolds. However, in the investigations of M theory, physicists encountered even exotic non-commutative structures beyond the conventional quantization schemes, including odd dimensional fuzzy spheres [8, 9, 10, 11]. From M(atr)ix theory point of view [12, 13], matrix geometries known as fuzzy manifolds [14, 15, 16, 17, 18, 19, 20, 21, 22, 23, 24, 25, 26] represent fundamental extended objects in the theory [27, 28]. Moreover, it has been recognized that the quantum Nambu algebra [29] plays crucial roles in the formulation of M theory (see Refs.[30, 31, 32] as nice reviews and references therein). It may be evident that a new non-commutative scheme is required to address these extraordinary non-commutative spaces that extend beyond the conventional quantization methods based on the commutator formalism.¹

Associated with the developments of the higher-dimensional quantum Hall effect, the understanding of higher-dimensional non-commutative geometry has significantly advanced in the past twenty years (see [39, 40] and references therein). We have learned that the higher dimensional non-commutative geometry on $\mathcal{M} \simeq G/H$ can be obtained by examining the Landau model on \mathcal{M} in the non-Abelian monopole background [41, 42, 43, 44, 45, 46, 47, 48, 49, 50, 51, 52]. Specifically, within the lowest Landau level, fuzzy manifolds \mathcal{M}_F were successfully realized. Nonetheless, it should be noticed that the underlying reason for the success is still missing. Furthermore, while the preceding analysis has provided a nice physical understanding of non-commutative geometries, one could argue that these analyses have not revealed unknown matrix geometries. Until now, substantial attention has been given to the geometry in the lowest Landau level; however, there is no logical reason for the exclusive presence of non-commutative geometry solely in this level. Indeed, it was demonstrated that the higher Landau levels also give rise to fuzzy geometries [53], which clearly shows that level projection to *any* Landau level generates non-commutativity. With regards to a two-sphere, the emergent non-commutative geometries of the higher Landau levels are the same as that of the lowest Landau level. In this sense, the geometry of higher Landau levels might not be so intriguing. Nevertheless, this does not rule out the possibility of discovering new non-commutative geometries in higher dimensional systems. Following this idea, explorations of novel quantum matrix geometries have been conducted in various Landau models, such as relativistic models and supersymmetric models [53], odd dimensional models [54] and even dimensional models [55, 56, 57]. It is also worthwhile to mention that quantum matrix geometries associated with the Berezin-Toeplitz quantization have been intensively studied in recent years [58, 59, 60, 61, 62, 63, 64].

Importantly, now the higher dimensional studies are not only relevant to theoretical interests but also to practical experiments. The idea of the synthetic dimension allows physicists to reach higher dimensional topological physics [65, 66, 67]. In particular, exotic topological effects of the non-Abelian monopole in higher dimension have already been observed through table top experiments very recently [68, 69, 70, 71]. It is expected that physical consequences arising from higher dimensional quantum geometry will be observed in these experimental systems.

In the present work, with an appropriate interpretation of the emergent non-commutative geometry

¹Interestingly, a cubit matrix realization is known for the quantum Nambu algebra [33, 34, 35], although we do not delve into such possibilities in this paper. The deformation quantization approach to the quantum Nambu geometry is also discussed in Refs.[36, 37, 38].

in the Landau models, we introduce a quantum-oriented non-commutative scheme that leverages Landau models as an effective “tool” to generate noble quantum geometries. Our approach provides a concrete prescription for generating the matrix geometry of the coset manifold $\mathcal{M} \simeq G/H$. It is shown that this scheme encompasses pure quantum Nambu matrix geometry, which cannot be described by conventional non-commutative methods. We also demonstrate that these quantum Nambu matrix geometries give rise to novel classical solutions in Yang-Mills matrix models.

This paper is organized as follows. In Sec.2, we revisit the derivation of the fuzzy two-sphere from the $SO(3)$ Landau model and address the underlying reasons behind the emergent non-commutative geometry of the Landau models. Sec.3 presents explicit fuzzy four-sphere matrix coordinates in the $SO(5)$ Landau levels. We investigate the matrix structures of fuzzy four-spheres and discuss their basic properties in Sec.4. In Sec.5, the nested internal structures of higher Landau level matrix geometries are exploited. We investigate the continuum limit and the classical geometry of the quantum matrix geometry using the coherent method and the probe brane method in Sec.6. In Sec.7, we demonstrate that the obtained quantum matrix geometries realize unexplored solutions of Yang-Mills matrix models and clarify their physical properties. Sec.9 is devoted to summary and discussions.

2 Quantum-oriented non-commutative scheme

In this section, we discuss the underlying mechanism behind the emergent matrix geometry in the simple $SO(3)$ Landau model and apply this observation to propose a prescription for generating matrix geometries of G/H .

2.1 Behind the scene of the emergent matrix geometry

The $SO(3)$ Landau model is a Landau model on S^2 and the Hamiltonian is given by

$$H = -\frac{1}{2M} \sum_{i=1}^3 (\partial_i + iA_i)^2|_{r=1}, \quad (1)$$

where A_i denotes the $U(1)$ gauge field of monopole at the origin:

$$A_i = -\frac{I}{2r(r+x_3)} \epsilon_{ij3} x_j. \quad (2)$$

The index $I/2$ signifies the monopole charge (In the following, we assume I to be a positive integer for simplicity). While the present system is originally investigated in [72, 73], we will utilize the concise notation of [53] in this paper. The eigenvalues of the Hamiltonian (1) are obtained as

$$E_N = \frac{1}{2M} (I(N + \frac{1}{2}) + N(N + 1)) \quad (N = 0, 1, 2, \dots), \quad (3)$$

and the corresponding eigenstates are given by the monopole harmonics

$$Y_m^{(N)}(\theta, \phi) = \sqrt{\frac{2N+I+1}{4\pi}} \mathcal{D}_{N+\frac{I}{2}}(\phi, -\theta, -\phi)_{\frac{I}{2}, m} \quad (m = N + \frac{I}{2}, N + \frac{I}{2} - 1, \dots, -(N + \frac{I}{2})), \quad (4)$$

where \mathcal{D} denotes the Wigner D-function:

$$\mathcal{D}_l(\chi, \theta, \phi) = e^{-i\chi S_z^{(l)}} e^{-i\theta S_y^{(l)}} e^{-i\phi S_z^{(l)}}. \quad (5)$$

Here, $S_i^{(l)}$ stand for the $SU(2)$ spin matrices with spin index l . We sandwich the coordinates on S^2 to derive the corresponding matrix coordinates:

$$(X_i^{(N)})_{mn} = \langle Y_m^{(N)} | x_i | Y_n^{(N)} \rangle \equiv \int_{S^2} d\theta d\phi \sin \theta Y_m^{(N)*} x_i Y_n^{(N)}, \quad (6)$$

where

$$x_1 = \cos \phi \sin \theta, \quad x_2 = \sin \phi \sin \theta, \quad x_3 = \cos \theta. \quad (7)$$

In the N th Landau level, $X_i^{[N]}$ are explicitly obtained as [53]

$$X_i^{(N)} = \frac{2I}{(I+2N)(I+2N+2)} S_i^{(\frac{I}{2}+N)}, \quad (8)$$

which satisfy

$$X_i^{(N)} X_i^{(N)} = \frac{I^2}{(I+2N)(I+2N+2)} \mathbf{1}_{I+2N+1}, \quad (9a)$$

$$[X_i^{(N)}, X_j^{(N)}] = i \frac{2I}{(I+2N)(I+2N+2)} \epsilon_{ijk} X_k^{(N)}. \quad (9b)$$

Equation (9) represents the algebra of fuzzy two-sphere [14]. Note that not only the lowest Landau level but also each of the higher Landau level matrix geometries realizes the fuzzy two-sphere matrix geometry.² The physical properties of (9) as a classical solution of Yang-Mills matrix models are discussed in Appendix B.

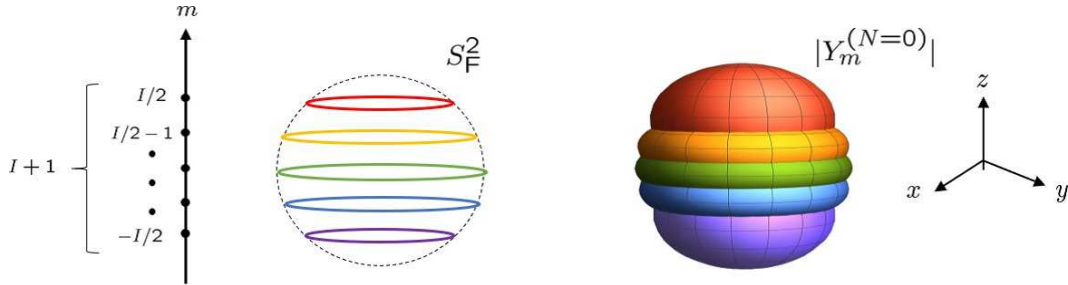


Figure 1: (left) The schematic picture of the fuzzy two-sphere for $N = 0$ (8). (right) The distributions of the magnitudes of the monopole harmonics, $|Y_m^{(N=0)}|$, of $m = I/2, I/2 - 1, \dots, -I/2$ for $I = 4$ are depicted as the red, orange, green, blue and violet orbitals, respectively. The monopole orbitals, $|Y_m^{(N=0)}|$, are localized around the latitudes $z = 2m/I$ on the two-sphere.

We depicted the fuzzy two-sphere and the magnitudes of the monopole harmonics in the left and the right of Fig.1, respectively. One may find an apparent resemblance between the left and the right pictures. The latitudes on the fuzzy two-sphere represent the degrees of freedom of the matrix geometry, *i.e.*, the “points”, in the fuzzy space. Obviously, each point on the fuzzy space corresponds to the monopole harmonics or each state of the $SU(2)$ irreducible representation. Therefore, one may consider the fuzzy two-sphere to be composed of the $SU(2)$ irreducible representation.

Reflecting the emergence of the non-commutative geometry, we can obtain the following insight.

1. About the role of global symmetry and irreducible representation:

The $SO(3)$ global symmetry of $S^2 \simeq SO(3)/SO(2)$ is naturally transformed to the $SU(2)$ symmetry on

²For completeness, we derive the non-commutative geometry in higher Landau levels of the planar Landau model in Appendix A.

the matrix geometry side introducing the projective representation of $SO(3)$. In the matrix geometry, an “uncertainty area” or a “point” corresponds to each state of the $SU(2)$ irreducible representation. The irreducible representation is “symmetric” in the sense that, while each state of an irreducible representation is transformed, the set of states in the irreducible representation remains unchanged under any $SU(2)$ transformation. In the language of matrix geometry, this means that fuzzy geometry also remains unchanged under $SU(2)$ transformations, as the fuzzy two-sphere is composed of the states in the $SU(2)$ irreducible representation. Moreover, the $SU(2)$ group is a compact group, and its irreducible representation is a finite-dimensional set with discrete quantum numbers, which aligns with the intuitive notion that a compact non-commutative space consists of finite-dimensional discrete points. In this way, while the fuzzy sphere is a discretized space, it realizes a space symmetric under *continuous* $SU(2)$ transformations, unlike the lattice space, which is symmetric only by the discrete translations corresponding to the lattice spacing. This is the specific feature of the matrix geometry composed of the irreducible representation.

2. About the role of the stabilizer group and the gauge symmetry:

The stabilizer group $SO(2)$ of $S^2 \simeq SO(3)/SO(2)$ is a subgroup of $SO(3)$ that does not change a point on the classical manifold S^2 [74]. A point in the classical geometry corresponds to a state of the irreducible representation on the matrix geometry side. Therefore, the stabilizer group is considered to be some transformation that does not change that state. The transformation that does not change physical state is nothing but a gauge transformation. To encapsulate, the stabilizer group represents redundant symmetry of the $SO(3)$ group in the classical system when representing $S^2 \simeq SO(3)/SO(2)$, and such redundancy is naturally regarded as a gauge symmetry on the quantum mechanical side. Consequently, the stabilizer group $SO(2)$ corresponds to the $U(1) \simeq SO(2)$ symmetry on the quantum mechanical side. It is interesting to see that while the stabilizer symmetry is an *external* symmetry on the classical mechanical side, it acts as the *internal* symmetry on the quantum mechanical side.³

3. Reinterpretation of the Landau model:

The above observations suggest that the matrix geometry corresponding to $S^2 \simeq SO(3)/SO(2)$ is obtained by considering a quantum system with global $SU(2)$ symmetry and $U(1)$ gauge symmetry. As we are dealing with the spatial manifold, the $U(1)$ gauge symmetry introduces the $U(1)$ *vector* potential whose field configuration should be compatible with the $SU(2)$ global symmetry. This necessarily leads to the radially symmetric magnetic field of the $U(1)$ monopole. Thus, the magnetic field is just a consequence of the gauge symmetry. In this way, we can reproduce the original $SO(3)$ Landau system. It is important to note that the *primary* significance lies in the gauge symmetry itself rather than the magnetic field, although the presence of a magnetic field is commonly believed to be essential for the emergence of non-commutative geometry.

These speculations provide a natural explanation for why the fuzzy two-sphere geometry has been successfully generated through the analyses of the $SO(3)$ Landau model.

2.2 Non-commutative scheme for generating the matrix geometry

With the above understanding, we now propose a prescription for obtaining the matrix geometry of the general coset manifold, $\mathcal{M} \simeq G/H$. We will utilize the quantum mechanics as a tool for generating matrix geometries. What we need to do is simply replace the $SO(3)$ in the above discussions with G and $SO(2)$

³This suggests that the external space and the internal space should be treated on the same footing in the matrix geometry [79].

with H .⁴

2.2.1 General prescription

1. Consider quantum mechanics with gauge symmetry H on base-manifold \mathcal{M} :

$$-\frac{1}{2M} \sum_a D_a^2 \Big|_{\mathcal{M}} \quad (10)$$

where $D_a = \partial_a + iA_a$ are covariant derivatives with the gauge field A_a of the gauge group H . The gauge field configuration has to be chosen to be compatible with the symmetry G of the base-manifold \mathcal{M} .

2. Solve the eigenvalue problem of the Hamiltonian (10) to derive the degenerate eigenstates of each energy level E_N :

$$|\psi_{N,\alpha}\rangle. \quad (11)$$

The set of degenerate eigenstates constitute an irreducible representation of G .⁵

3. Derive the matrix elements of the coordinates x_a of \mathcal{M} utilizing (11) to construct the matrix coordinates of $\mathcal{M}_F^{(N)}$:

$$(X_a^{(N)})_{\alpha\beta} = \langle \psi_{N,\alpha} | x_a | \psi_{N,\beta} \rangle \equiv \int_{\mathcal{M}} d\Omega \psi_{N,\alpha}^\dagger x_a \psi_{N,\beta}, \quad (12)$$

where $d\Omega$ is the area element of \mathcal{M} .

Notice each energy level N hosts its own matrix geometry $X_a^{[N]}$, and distinct energy levels yield different quantum matrix coordinates in general. Consequently, multiple quantum geometries will be obtained from a single classical manifold. The flow of this procedure is depicted in Fig.2.

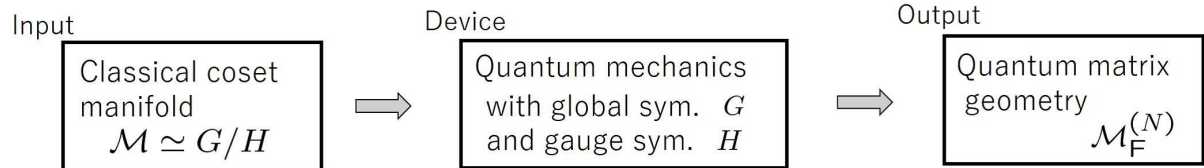


Figure 2: Flow of the procedure.

2.2.2 Advantages

Here, we will outline the advantages of the present construction.

1. The first merit is that we do not need to worry about mathematical inconsistency. In the present scheme, non-commutative geometry is not postulated a priori but is what emerges in each of the energy levels. As the original quantum system is totally physical and the existence of mathematically consistent Hilbert space behind the quantum mechanics is founded, there is no need to be concerned about mathematical inconsistencies.⁶

⁴While we will assume that G is a compact group with finite dimensional irreducible representations, our discussions can also be applied to non-compact groups with discrete series of infinite dimensional irreducible representations [26].

⁵In general, the Hamiltonian may possess symmetries other than G . In such a case, the degenerate eigenstates constitute states of an irreducible representation of the entire symmetry. See Sec.5.2.

⁶This is inspired by the idea of Ref.[75].

2. Following the above simple prescription, we can mechanically derive matrix geometries for *arbitrary* classical manifolds of the type $\mathcal{M} \simeq G/H$. Notably, odd dimensional manifolds are also within the realm of this scheme. Therefore, this scheme is not restricted to the symplectic manifolds unlike the conventional quantization methods in which the quantization is basically executed by replacing the Poisson bracket with the commutator. This suggests that the present scheme is beyond the non-commutative geometry based on the canonical commutator formalism.
3. The present non-commutative scheme is primarily based on irreducible representations of quantum mechanics. In this sense, this may be referred to as a quantum-oriented scheme. The emergent matrix geometries may even encompass pure quantum geometries that do not have their classical counterparts. We may explore quantum geometries that have eluded in the conventional non-commutative schemes.

2.3 General Properties

To examine specific properties of the present scheme, let us consider even dimensional spheres,

$$S^{2k} \simeq SO(2k+1)/SO(2k). \quad (13)$$

2.3.1 Covariance

We assume that the global symmetry $SO(2k+1)$ of S^{2k} is given by

$$x_{a=1,2,\dots,2k+1} \rightarrow R_{ab}x_b \quad (R_{ab} \in SO(2k+1)). \quad (14)$$

The stabilizer group is defined so that the condition $x_a = \delta_{a,2k+1}$ does not change, which is the $SO(2k)$ transformation:

$$x_{\mu=1,2,\dots,2k} \rightarrow R_{\mu\nu}x_\nu \quad (R_{\mu\nu} \in SO(2k)). \quad (15)$$

Transformations (14) and (15) respectively correspond to the following transformations on the quantum mechanics side:

$$|\psi_\alpha^{(i)}\rangle \rightarrow |\psi_\beta^{(i)}\rangle U_{\beta\alpha} \quad (U \in Spin(2k+1)), \quad (16)$$

and

$$|\psi_\alpha^{(i)}\rangle \rightarrow g_{ij}|\psi_\alpha^{(j)}\rangle \quad (g \in Spin(2k)). \quad (17)$$

Equation (16) stands for the global transformation, and α denote the index of the irreducible representation of the $Spin(2k+1)$. Similarly, Eq.(17) represents the gauge transformation, and i signify that of the gauge group $Spin(2k)$. Under these transformations, X_a behave as

$$(X_a)_{\alpha\beta} = \sum_i \langle \psi_\alpha^{(i)} | x_a | \psi_\beta^{(i)} \rangle \rightarrow \sum_i U_{\alpha'\alpha}^* \langle \psi_{\alpha'}^{(i)} | x_a | \psi_{\beta'}^{(i)} \rangle U_{\beta'\beta} = (U^\dagger X_a U)_{\alpha\beta} = R_{ab}(X_b)_{\alpha\beta}, \quad (18)$$

and

$$(X_a)_{\alpha\beta} = \sum_i \langle \psi_\alpha^{(i)} | x_a | \psi_\beta^{(i)} \rangle \rightarrow \sum_{j,k} \overbrace{\sum_i g_{ij}^* g_{ik}}^{=\delta_{jk}} \langle \psi_\alpha^{(j)} | x_a | \psi_\beta^{(k)} \rangle = \sum_j \langle \psi_\alpha^{(j)} | x_a | \psi_\beta^{(j)} \rangle = (X_a)_{\alpha\beta}. \quad (19)$$

The matrix coordinates thus transform as the $SO(2k+1)$ vector, similar to the classical coordinates on S^{2k} , and they are gauge invariant. Generally for $\mathcal{M} \simeq G/H$, the matrix coordinates are H gauge invariant and transform under G in the same way as the classical coordinates of the original manifold \mathcal{M} .

2.3.2 Beyond the commutator formalism

In the well known construction of the fuzzy $2k$ -sphere [16, 15], the matrix coordinates are given by the totally symmetric combination of the gamma matrices, which satisfy the following commutation relations

$$[X_a, X_b] = 4i\Sigma_{ab}, \quad (20a)$$

$$[X_a, \Sigma_{bc}] = -i\delta_{ab}X_c + i\delta_{ac}X_b, \quad (20b)$$

$$[\Sigma_{ab}, \Sigma_{cd}] = i\delta_{ac}\Sigma_{bd} - i\delta_{ad}\Sigma_{bc} + i\delta_{bd}\Sigma_{ac} - i\delta_{bc}\Sigma_{ad}. \quad (20c)$$

The commutators of X_a yield new matrices Σ_{ab} (20a), which are the generators of $SO(2k+1)$. In total, X_a and Σ_{ab} together form the $SO(2k+2)$ algebra. Such a matrix geometry is known to emerge in the lowest Landau level of the $SO(2k+1)$ Landau model [79]. The lowest Landau level matrix geometry is well described by the commutator formalism. On the other hand, for the higher Landau levels, some subtleties occur. The $SO(2k+1)$ angular momentum operators in the $SO(2k)$ monopole background are constructed as [44]

$$L_{ab} = -ix_a(\partial_b + iA_b) + ix_b(\partial_a + iA_a) + \frac{1}{r^2}F_{ab}, \quad (21)$$

which satisfy the $SO(2k+1)$ algebra:

$$[L_{ab}, L_{cd}] = i\delta_{ac}L_{bd} - i\delta_{ad}L_{bc} + i\delta_{bd}L_{ac} - i\delta_{bc}L_{ad}. \quad (22)$$

Since the coordinates x_a on S^{2k} transform as an $SO(2k+1)$ vector, the algebra associated with the $SO(2k+1)$ transformation is represented as

$$[x_a, L_{bc}] = -i\delta_{ab}x_c + i\delta_{ac}x_b. \quad (23)$$

Let us construct matrix coordinates for a given irreducible representation of $SO(2k+1)$, $\{\psi_1^{(r)}, \psi_2^{(r)}, \dots, \psi_{D(r)}^{(r)}\}$:

$$(X_a^{(r)})_{\alpha\beta} \equiv \langle \psi_\alpha^{(r)} | x_a | \psi_\beta^{(r)} \rangle, \quad (\Sigma_{ab}^{(r)})_{\alpha\beta} \equiv \langle \psi_\alpha^{(r)} | L_{ab} | \psi_\beta^{(r)} \rangle. \quad (24)$$

It is important to note that the completeness relation holds for the total set of the irreducible representations:

$$\sum_r \sum_{\alpha=1}^{D(r)} |\psi_\alpha^{(r)}\rangle \langle \psi_\alpha^{(r)}| = 1, \quad (25)$$

but *not* for each individual irreducible representation:

$$\sum_{\alpha=1}^{D(r)} |\psi_\alpha^{(r)}\rangle \langle \psi_\alpha^{(r)}| \neq 1. \quad (26)$$

Equation (26) is a direct consequence of the level projection which is the heart of non-commutative geometry [53]. Due to Eq.(26), $X_a^{(r)}$ (24) generally become non-commutative matrices, whereas the original coordinates x_a are commutative quantities. From the property of the irreducible representation

$$\langle \psi_\alpha^{(r)} | L_{ab} | \psi_\beta^{(r')} \rangle = (\Sigma_{ab}^{(r)})_{\alpha\beta} \delta_{rr'}, \quad (27)$$

one may easily reproduce the lower two equations of (20) using Eqs.(22) and (23). On the other hand, unlike Eq.(27), the matrix coordinates are not completely block diagonalized, $\langle \psi_\alpha^{(r)} | x_a | \psi_\beta^{(r')} \rangle \neq \langle \psi_\alpha^{(r)} | x_a | \psi_\beta^{(r)} \rangle \delta_{rr'}$ (see Sec.3.1 for more details). Consequently, the first relation (20a) turns out to be questionable,

$$[X_a^{(r)}, X_b^{(r)}] \stackrel{?}{\propto} i\Sigma_{ab}^{(r)}. \quad (28)$$

Equation (20a) is not guaranteed in general. So, if the Lie algebraic geometry fails, what kind of geometry will emerge? That is the topic that we shall discuss in Sec.4 and Sec.8. The failure of Eq.(20a) implies that the present scheme is beyond the realm of the conventional commutator formalism.

Here, we also mention relationship to the Berezin-Toeplitz quantization. The Berezin-Toeplitz quantization is a method that maps a function to a finite dimensional matrix [76, 62, 5]. In this sense, the Berezin-Toeplitz quantization shares the same spirit with the present scheme. However, Berezin-Toeplitz quantization is primarily concerned with symplectic manifolds and is based on commutator formalism. The Kernel employed in the Berezin-Toeplitz quantization corresponds to the zero-modes of the Dirac-Landau operator whose zero-modes are essentially equivalent to the lowest Landau level eigenstates [55, 53]. Therefore, the Berezin-Toeplitz quantization is thus closely related to the lowest Landau level matrix geometry and can be viewed as a special case of the present scheme.⁷ We will revisit this in Sec.4.

3 Matrix coordinates from the $SO(5)$ Landau model

In this section, we will directly apply the present scheme to generate quantum matrix geometries for S^4 . Using the $SO(5)$ Landau model, we will derive the complete form of matrix coordinates in arbitrary Landau levels. This section also includes a review of Ref.[55].

3.1 The $SO(5)$ Landau model

Since $S^4 \simeq SO(5)/SO(4)$, we need to consider a quantum mechanics on S^4 with $Spin(4)$ gauge degrees of freedom. For the $Spin(4)$ gauge field configuration to respect the $SO(5)$ global symmetry of S^4 , we place a $Spin(4)$ monopole at the origin. While the Landau model in such a $Spin(4)$ monopole background has been investigated [57], we will consider a simpler system by taking one $SU(2)$ from the $Spin(4) \simeq SU(2) \otimes SU(2)$. In the following, we then consider a quantum mechanics on S^4 in the $SU(2)$ monopole background, which was originally introduced in Refs.[77, 78, 41].

Let us briefly discuss such a $SO(5)$ Landau model with a modern notation [55]. The $SO(5)$ Landau Hamiltonian is given by

$$H = -\frac{1}{2M} \sum_{a=1}^5 D_a^2|_{r=0} = \frac{1}{2M} \sum_{a<b} \Lambda_{ab}^2 \quad (29)$$

where $D_a = \partial_a + iA_a$ and

$$\Lambda_{ab} = -ix_a D_b + ix_b D_a. \quad (30)$$

The gauge field is chosen to be Yang's $SU(2)$ monopole:

$$A_{\mu=1,2,3,4} = -\frac{1}{r(r+x_5)} \bar{\eta}_{\mu\nu}^i x_\nu S_i^{(I/2)}, \quad A_5 = 0, \quad (I = 1, 2, 3, \dots) \quad (31)$$

with $\bar{\eta}_{\mu\nu}^i = \epsilon_{\mu\nu i 4} - \delta_{\mu i} \delta_{\nu 4} + \delta_{\nu i} \delta_{\mu 4}$. The $SO(5)$ Landau Hamiltonian is equal to the $SO(5)$ Casimir up to a constant. Consequently, the energy eigenvalues are specified by two indices of the $SO(5)$ Casimir, $(p, q)_5 = (N + I, N)_5$. The $SO(5)$ Landau levels are explicitly given by

$$E_N = \frac{1}{2M} ((N + 1)I + N(N + 3)) \quad (N = 0, 1, 2, \dots). \quad (32)$$

The eigenstates of each of the Landau levels form an irreducible representation of $SO(5)$ and are referred to as the $SO(5)$ monopole harmonics in this paper⁸ to emphasize its $SO(5)$ covariance. We parameterize

⁷Recently mathematicians are also interested in higher Landau levels from the perspective of the Berezin-Toeplitz quantization [86, 87].

⁸In the original paper [78], they are referred to as the $SU(2)$ monopole harmonics.

the coordinates of the four-sphere with a unit radius as

$$x_{\mu=1,2,3,4} = \sin \xi \, y_{\mu}, \quad x_5 = \cos \xi \quad \left(\sum_{\mu=1}^4 y_{\mu} y_{\mu} = 1 \right), \quad (33)$$

where ξ represents the azimuthal angle and y_m denote the coordinates of (normalized) S^3 -hyper-latitude:

$$y_1 = \sin \chi \sin \theta \cos \phi, \quad y_2 = \sin \chi \sin \theta \sin \phi, \quad y_3 = \sin \chi \cos \theta, \quad y_4 = \cos \chi. \quad (34)$$

Normalized $SO(5)$ monopole harmonics are represented as

$$\Psi_{N;j,m_j;k,m_k}(\xi, \chi, \theta, \phi) = G_{N,j,k}(\xi) \cdot \mathbf{Y}_{j,m_j;k,m_k}(\chi, \theta, \phi), \quad (35)$$

where

$$G_{N,j,k}(\xi) = (-1)^{2j+1} \sqrt{N + \frac{I}{2} + \frac{3}{2}} \frac{1}{\sin \xi} d_{N+\frac{I}{2}+1, -j+k, j+k+1}(\xi), \quad (36a)$$

$$\mathbf{Y}_{j,m_j;k,m_k}(\chi, \theta, \phi) = \sum_{m_R=-j}^j \begin{pmatrix} C_{j,m_R;\frac{I}{2},\frac{I}{2}}^{k,m_k} \Phi_{j,m_j;j,m_R}(\chi, \theta, \phi) \\ C_{j,m_R;\frac{I}{2},\frac{I}{2}-1}^{k,m_k} \Phi_{j,m_j;j,m_R}(\chi, \theta, \phi) \\ \vdots \\ C_{j,m_R;\frac{I}{2},-\frac{I}{2}}^{k,m_k} \Phi_{j,m_j;j,m_R}(\chi, \theta, \phi) \end{pmatrix}. \quad (36b)$$

Here, $d_{l,m,m'}(\xi) \equiv \mathcal{D}_l(0, \xi, 0)_{m,m'}$ in (36a) stand for Wigner's small D -matrices, C s in (36b) represent the Clebsch-Gordan coefficients, and Φ s in (36b) denote the $SO(4)$ spherical harmonics [54]. The $SO(5)$ monopole harmonics satisfy

$$\int_{S^4} d\Omega_4 \, \Psi_{N;j,m_j;k,m_k}^\dagger \Psi_{N';j',m'_j;k',m'_k} = \delta_{N,N'} \delta_{j,j'} \delta_{k,k'} \delta_{m_j,m'_j} \delta_{m_k,m'_k} \quad (37)$$

and

$$\sum_{n=0}^N \sum_{s=-I/2}^{I/2} \sum_{m_j=-j}^j \sum_{m_k=-k}^k \Psi_{N;j,m_j;k,m_k} \Psi_{N;j,m_j;k,m_k}^\dagger = \frac{(N+1)(I+N+2)(I+2N+3)}{16\pi^2} \mathbf{1}_{I+1}, \quad (38)$$

where $d\Omega_4 \equiv d\xi d\chi d\theta d\phi \sin^3 \xi \sin^2 \chi \sin \theta$.

The $SO(5)$ irreducible representation $(p, q)_5 = (N+I, N)_5$ is decomposed as (see Fig.3)

$$(N+I, N)_5 = \bigoplus_{n=0}^N (n) = \bigoplus_{n=0}^N \bigoplus_{s=-I/2}^{I/2} (j, k)_4, \quad (39)$$

where

$$(n) \equiv \bigoplus_{s=-I/2}^{I/2} (j, k)_4 \quad (40)$$

signifies the set of the $SO(4)$ irreducible representations in the $SO(4)$ line (the oblique line of the same color in Fig.3). The N th $SO(5)$ Landau level eigenstates consist of $SO(4)$ irreducible representations on the $SO(4)$ lines with $n = 0, 1, 2, \dots, N$. The $SO(4)$ bi-spin index, $(j, k)_4$, is defined as

$$(j, k)_4 \equiv \left(\frac{n}{2} + \frac{I}{4} + \frac{s}{2}, \frac{n}{2} + \frac{I}{4} - \frac{s}{2} \right)_4, \quad (41)$$

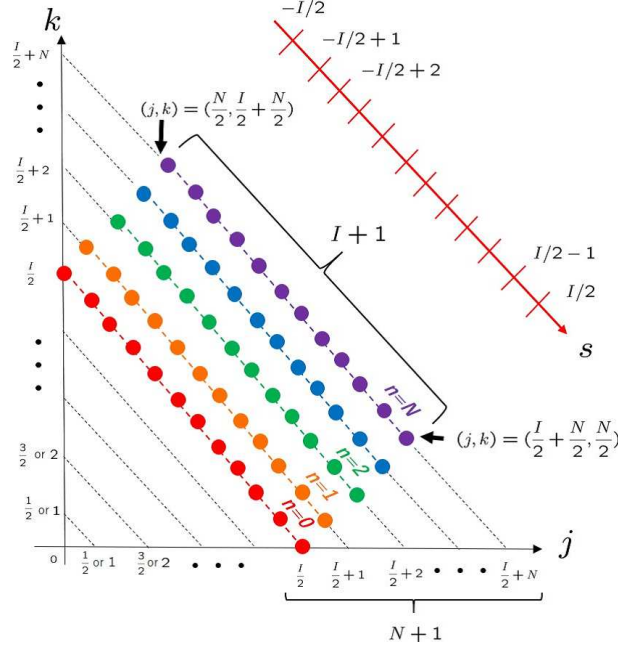


Figure 3: Each of the filled circles represents an $SO(4)$ irreducible representation (j, k) . The $SO(4)$ irreducible representations denoted by the filled circles amount to the $SO(5)$ irreducible representation $(p, q)_5 = (N + I, N)_5$. (Taken from [55].)

with

$$n = 0, 1, 2, 3, \dots, N, \quad s = \frac{I}{2}, \frac{I}{2} - 1, \dots, -\frac{I}{2}. \quad (42)$$

The dimension of the $SO(4)$ irreducible representation (41) is given by

$$d(n, I, s) = (2j + 1)(2k + 1) = (n + \frac{I}{2} + s + 1)(n + \frac{I}{2} - s + 1) = d(n, I, -s), \quad (43)$$

and that of the $SO(4)$ line is

$$d(n, I) \equiv \sum_{s=-I/2}^{I/2} d(n, I, s) = \frac{1}{6}(I + 1)(I^2 + (6n + 5)I + 6(n + 1)^2). \quad (44)$$

Consequently, the N th Landau level degeneracy is counted as

$$D(N, I) = \sum_{n=0}^N d(n, I) = \sum_{n=0}^N \sum_{s=-I/2}^{I/2} d(n, I, s) = \frac{1}{6}(N + 1)(I + 1)(I + N + 2)(I + 2N + 3). \quad (45)$$

3.2 Matrix coordinates

The matrix coordinates have non-zero components only within the same Landau level and among adjacent Landau levels [55]:

$$\langle x_5 \rangle \neq 0 \rightarrow \Delta N = 0, \quad (46a)$$

$$\langle x_\mu \rangle \neq 0 \rightarrow \Delta N = 0, \pm 1. \quad (46b)$$

See the left of Fig.4 where the non-zero matrix elements are denoted as the shaded color regions. Under the $SO(4)$ rotation around the fifth axis, x_5 behaves as a scalar $(j, k) = (0, 0)$, while x_μ transform as a bi-spinor $(j, k) = (1/2, 1/2)$. From (41), we can see that the $SO(4)$ selection rule implies that non-zero matrix coordinates exist only for

$$X_5^{[N]} \neq 0 \rightarrow (\Delta n, \Delta s) = (0, 0), \quad (47a)$$

$$X_\mu^{[N]} \neq 0 \rightarrow (\Delta n, \Delta s) = (\pm 1, 0), \quad (0, \pm 1). \quad (47b)$$

Equation (47a)/(47b) corresponds to the upper/lower right of Fig.4. There are two cases in which $X_\mu^{[N]}$ take finite values. The first is $(\Delta n, \Delta s) = (\pm 1, 0)$ that corresponds to the green shaded rectangles in Fig.4, representing transitions between two adjacent $SO(4)$ lines in Fig.3. The second $(\Delta n, \Delta s) = (0, \pm 1)$ corresponds to the small purple shaded rectangles in Fig.4, signifying transitions between two adjacent $SO(4)$ irreducible representations on same $SO(4)$ lines in Fig.3. With this in mind, we will explicitly evaluate the matrix elements of x_a .

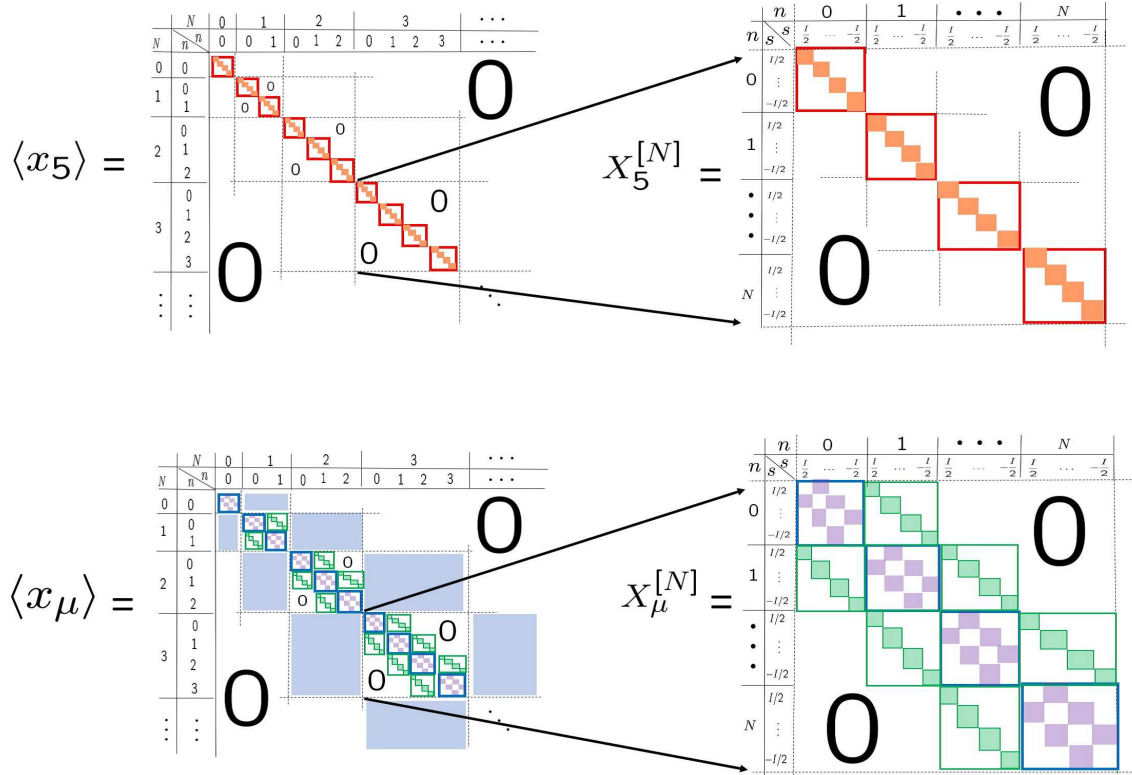


Figure 4: The matrix coordinate representation of x_a .

We can perform integrations of the azimuthal part and the S^3 -hyper-latitude part separately. For instance, the ortho-normal condition (37) is evaluated as

$$\langle \Psi_{N';j',m'_j;k',m'_k} | \Psi_{N;j,m_j;k,m_k} \rangle = \langle G_{N',j',k'} | G_{N,j,k} \rangle \cdot \langle Y_{j',m'_j;k',m'_k} | Y_{j,m_j;k,m_k} \rangle, \quad (48)$$

where

$$\langle G_{N',j,k} | G_{N,j,k} \rangle = \int_0^\pi d\xi \sin^3 \xi \, G_{N,j,k}(\xi)^* G_{N',j,k}(\xi) = \delta_{N,N'}, \quad (49a)$$

$$\langle Y_{j',m'_j;k',m'_k} | Y_{j,m_j;k,m_k} \rangle = \int_{S^3} d\chi d\theta d\phi \, \sin^2 \chi \, \sin \theta \, \mathbf{Y}_{j,m_j;k,m_k}(\chi, \theta, \phi)^\dagger \mathbf{Y}_{j',m'_j;k',m'_k}(\chi, \theta, \phi) = \delta_{jj'} \delta_{m_j m'_j} \delta_{kk'} \delta_{m_k m'_k}. \quad (49b)$$

The matrix elements of $X_5^{[N]}$ are derived as⁹

$$X_5^{[N]} : -\langle \Psi_{N;j',m'_j;k',m'_k} | x_5 | \Psi_{N;j,m_j;k,m_k} \rangle = -\langle G_{N,j,k} | x_5 | G_{N,j,k} \rangle \cdot \delta_{j,j'} \delta_{k,k'} \delta_{m_j,m'_j} \delta_{m_k,m'_k}, \quad (50)$$

where

$$-\langle G_{N,j,k} | x_5 | G_{N,j,k} \rangle = \frac{2n + I + 2}{(2N + I + 2)(2N + I + 4)} \cdot 2s. \quad (51)$$

The matrix coordinate (51) takes equally spaced discrete values specified by $s = I/2, I/2 - 1, \dots, -I/2$, which are regarded as the hyper-latitudes on fuzzy four-sphere. This structure is quite similar to that of the fuzzy two-sphere (Fig.1). However notice that while the latitudes of fuzzy two-sphere are not degenerate, the hyper-latitudes of fuzzy four-sphere are degenerate, resulting in an intriguing internal structure as we shall discuss in Sec.5. Next, we turn to

$$\begin{aligned} X_\mu^{[N]} : & \langle \Psi_{N;j',m'_j;k',m'_k} | x_\mu | \Psi_{N;j,m_j;k,m_k} \rangle \\ &= \sum_{\sigma, \tau = +, -} \langle G_{N,j+\frac{\sigma}{2},k+\frac{\tau}{2}} | \sin \xi | G_{N,j,k} \rangle \langle Y_{j+\frac{\sigma}{2},m'_j;k+\frac{\tau}{2},m'_k} | y_\mu | Y_{j,m_j;k,m_k} \rangle \delta_{j',j+\frac{\sigma}{2}} \delta_{k',k+\frac{\tau}{2}}. \end{aligned} \quad (52)$$

Here, the azimuthal part is evaluated as

$$\langle G_{N,j+\frac{\sigma}{2},k+\frac{\tau}{2}} | \sin \xi | G_{N,j,k} \rangle = \delta_{\sigma,\tau} \langle G_{N,j+\frac{\sigma}{2},k+\frac{\sigma}{2}} | \sin \xi | G_{N,j,k} \rangle + \delta_{\sigma,-\tau} \langle G_{N,j+\frac{\sigma}{2},k-\frac{\sigma}{2}} | \sin \xi | G_{N,j,k} \rangle, \quad (53)$$

with¹⁰

$$\begin{aligned} \langle G_{N,j+\frac{\sigma}{2},k+\frac{\sigma}{2}} | \sin \xi | G_{N,j,k} \rangle &= -\frac{4s}{(2N + I + 2)(2N + I + 4)} \sqrt{(N - n + \frac{1-\sigma}{2})(N + n + I + 2 + \frac{1+\sigma}{2})}, \\ \langle G_{N,j+\frac{\sigma}{2},k-\frac{\sigma}{2}} | \sin \xi | G_{N,j,k} \rangle &= -\frac{4n + 2I + 4}{(2N + I + 2)(2N + I + 4)} \sqrt{(N + \frac{I}{2} - \sigma s + 1)(N + \frac{I}{2} + \sigma s + 2)}. \end{aligned} \quad (55)$$

⁹The minus sign in (50) is not essential but added for later convenience.

¹⁰In the derivation of (53), we used the formulas,

$$\int_0^\pi d\theta \, \sin \theta \, d_{l,m',n}(\theta) \, \sin \theta \, d_{l,m,n}(\theta) |_{m'=m\pm 1} = \frac{2n}{(2l+1)(l+1)l} \sqrt{(l \pm m + 1)(l \mp m)}, \quad (54a)$$

$$\int_0^\pi d\theta \, \sin \theta \, d_{l,m,n'}(\theta) \, \sin \theta \, d_{l,m,n}(\theta) |_{n'=n\pm 1} = -\frac{2m}{(2l+1)(l+1)l} \sqrt{(l \pm n + 1)(l \mp n)}. \quad (54b)$$

The S^3 -hyper-latitude part is

$$\begin{aligned}
\langle Y_{j+\frac{\sigma}{2}, m'_j; k+\frac{\tau}{2}, m'_k} | y_1 | Y_{j, m_j; k, m_k} \rangle &= \frac{\sqrt{(2j+1)(2k+1)}}{2} (-1)^{n+I+\frac{\tau}{2}} \begin{Bmatrix} j+\frac{\sigma}{2} & k+\frac{\tau}{2} & \frac{I}{2} \\ k & j & \frac{1}{2} \end{Bmatrix} \sum_{\kappa=+,-} (-1)^{\frac{\kappa-1}{2}} C_{\frac{1}{2}, \frac{\kappa}{2}; j, m_j}^{j+\frac{\sigma}{2}, m'_j} C_{\frac{1}{2}, \frac{\kappa}{2}; k, m_k}^{k+\frac{\tau}{2}, m'_k}, \\
\langle Y_{j+\frac{\sigma}{2}, m'_j; k+\frac{\tau}{2}, m'_k} | y_2 | Y_{j, m_j; k, m_k} \rangle &= -i \frac{\sqrt{(2j+1)(2k+1)}}{2} (-1)^{n+I+\frac{\tau}{2}} \begin{Bmatrix} j+\frac{\sigma}{2} & k+\frac{\tau}{2} & \frac{I}{2} \\ k & j & \frac{1}{2} \end{Bmatrix} \sum_{\kappa=+,-} C_{\frac{1}{2}, \frac{\kappa}{2}; j, m_j}^{j+\frac{\sigma}{2}, m'_j} C_{\frac{1}{2}, \frac{\kappa}{2}; k, m_k}^{k+\frac{\tau}{2}, m'_k}, \\
\langle Y_{j+\frac{\sigma}{2}, m'_j; k+\frac{\tau}{2}, m'_k} | y_3 | Y_{j, m_j; k, m_k} \rangle &= -\frac{\sqrt{(2j+1)(2k+1)}}{2} (-1)^{n+I+\frac{\tau}{2}} \begin{Bmatrix} j+\frac{\sigma}{2} & k+\frac{\tau}{2} & \frac{I}{2} \\ k & j & \frac{1}{2} \end{Bmatrix} \sum_{\kappa=+,-} C_{\frac{1}{2}, \frac{\kappa}{2}; j, m_j}^{j+\frac{\sigma}{2}, m'_j} C_{\frac{1}{2}, -\frac{\kappa}{2}; k, m_k}^{k+\frac{\tau}{2}, m'_k}, \\
\langle Y_{j+\frac{\sigma}{2}, m'_j; k+\frac{\tau}{2}, m'_k} | y_4 | Y_{j, m_j; k, m_k} \rangle &= i \frac{\sqrt{(2j+1)(2k+1)}}{2} (-1)^{n+I+\frac{\tau}{2}} \begin{Bmatrix} j+\frac{\sigma}{2} & k+\frac{\tau}{2} & \frac{I}{2} \\ k & j & \frac{1}{2} \end{Bmatrix} \sum_{\kappa=+,-} (-1)^{\frac{\kappa-1}{2}} C_{\frac{1}{2}, \frac{\kappa}{2}; j, m_j}^{j+\frac{\sigma}{2}, m'_j} C_{\frac{1}{2}, -\frac{\kappa}{2}; k, m_k}^{k+\frac{\tau}{2}, m'_k},
\end{aligned} \tag{56}$$

where $C_{\frac{1}{2}, \frac{\kappa}{2}; j, m}^{j+\frac{\sigma}{2}, m'}$ denote the Clebsch-Gordan coefficients:

$$C_{\frac{1}{2}, \frac{\kappa}{2}; j, m}^{j+\frac{\sigma}{2}, m'} = \delta_{m', m+\frac{\sigma}{2}} \left(\delta_{\tau, 1} \sqrt{\frac{j+\kappa m+1}{2j+1}} + \kappa \delta_{\tau, -1} \sqrt{\frac{j+\kappa m}{2j+1}} \right). \tag{57}$$

The formulas of Appendix D in [55] were utilized in the derivation of Eq.(56). We thus derived the explicit form of the matrix coordinates in the $SO(5)$ Landau levels. For a better understanding, in Appendix C, we provide the matrix coordinates for the case of $(N, I) = (1, 1)$. Note that all of the quantities involved in the matrix coordinate calculations, such as an integral measure and S^4 coordinates, are $SO(5)$ invariant or covariant quantities. Consequently, the obtained matrix coordinates are necessarily $SO(5)$ covariant coordinates that transform as the $SO(5)$ vector like the original S^4 coordinates (see Eq.(86)).

In the case of $I = 0$, the gauge symmetry no longer exists. Therefore, we cannot expect fuzzy geometries (recall that the gauge symmetry is crucial in the present scheme). Indeed, when $I = 0$, the energy eigenstates are given by the $SO(5)$ spherical harmonics and the matrix coordinates become trivial:

$$X_a^{[N]} = 0. \tag{58}$$

The corresponding dimensions of the $SO(5)$ spherical harmonics are

$$D(N, I = 0) = \frac{1}{6}(N+1)(N+2)(2N+3) = 5, 14, 30, \dots \tag{59}$$

Therefore in these matrix dimensions, the matrix geometries do not exist. In Ref.[16], the authors argued the non-existence of five-dimensional matrix coordinates, which corresponds to the smallest dimension in Eq.(59).

4 Pure quantum Nambu matrix geometry

Using the explicit matrix coordinates, we now expand concrete discussions about the matrix geometries. It is shown that the matrix coordinates satisfy

$$\sum_{a=1}^5 X_a^{[N]} X_a^{[N]} = c_1(N, I) \mathbf{1} \tag{60}$$

and

$$[X_a^{[N]}, X_b^{[N]}, X_c^{[N]}, X_d^{[N]}] = 4! c_3(N, I) \sum_{e=1}^5 \epsilon_{abcde} X_e^{[N]}, \tag{61}$$

where the quantum Nambu bracket denotes the totally antisymmetric combination of the four-quantities inside the bracket:

$$[O_1, O_2, O_3, O_4] \equiv \text{sgn}(\sigma) O_{\sigma_1} O_{\sigma_2} O_{\sigma_3} O_{\sigma_4}. \quad (62)$$

(Detail discussions about the coefficients, c_1 and c_3 , will be given in Sec.4.2.) Equations (60) and (61) signify a realization of the fuzzy four-sphere [16, 15]. The quantum Nambu geometry thus emerges as the matrix geometry in the $SO(5)$ Landau levels. We delve into geometric structures hidden in the mathematics of the quantum Nambu algebra using the explicit form of the matrix coordinates.

4.1 The lowest Landau level matrix geometry

For $N = 0$, Eqs.(50) and (52) reproduce the lowest Landau level matrix coordinates previously obtained in [55, 60]:

$$X_a^{[0]} = \frac{1}{I+4} \Gamma_a, \quad (63)$$

where Γ^a represent the I -fold symmetric tensor product of the $SO(5)$ gamma matrices [16]:

$$\Gamma^a = (\gamma^a \otimes 1 \otimes \cdots \otimes 1 + 1 \otimes \gamma^a \otimes \cdots \otimes 1 + \cdots + 1 \otimes 1 \otimes \cdots \otimes \gamma^a)_{\text{sym}} \quad (64)$$

with

$$\gamma_i = \begin{pmatrix} 0 & i\sigma_i \\ -i\sigma_i & 0 \end{pmatrix}, \quad \gamma_4 = \begin{pmatrix} 0 & 1_2 \\ 1_2 & 0 \end{pmatrix}, \quad \gamma_5 = \begin{pmatrix} 1_2 & 0 \\ 0 & -1_2 \end{pmatrix}. \quad (65)$$

We can readily check that $X_a^{[0]}$ satisfy (60) and (61),

$$\sum_{a=1}^5 X_a^{[0]} X_a^{[0]} = \frac{I}{I+4} \mathbf{1}_{\frac{1}{8}(I+1)(I+2)(I+3)} \quad (66)$$

and

$$[X_a^{[0]}, X_b^{[0]}, X_c^{[0]}, X_d^{[0]}] = -(I+2) \left(\frac{2}{I+4} \right)^3 \epsilon_{abcde} X_e^{[0]}. \quad (67)$$

The radius and the non-commutative scale are derived as

$$\begin{aligned} R &= \sqrt{\frac{I}{I+4}} \quad (I \xrightarrow{\infty} 1), \\ \Delta X &= \frac{2}{I+4} \quad (I \xrightarrow{\infty} 0), \end{aligned} \quad (68a)$$

which implies that the ordinary four-sphere with a unit radius is reproduced in the continuum limit (Fig.5).

It should be emphasized that the algebra of X_a can be described within the commutator formalism, and the quantum Nambu algebra (67) is not indispensable for the description of the lowest Landau level matrix geometry. The matrix coordinates $X_a^{[0]}$ and $X_{ab}^{[0]} \equiv -i\frac{1}{4}[X_a^{[0]}, X_b^{[0]}]$ satisfy a closed algebra

$$\begin{aligned} [X_a^{[0]}, X_b^{[0]}] &= 4i \frac{1}{(I+4)^2} X_{a,b}^{[0]}, \quad [X_a^{[0]}, X_{bc}^{[0]}] = -i\delta_{ab} X_c^{[0]} + i\delta_{ac} X_b^{[0]}, \\ [X_{ab}^{[0]}, X_{cd}^{[0]}] &= i\delta_{ac} X_{bd}^{[0]} - i\delta_{ad} X_{bc}^{[0]} + i\delta_{bd} X_{ac}^{[0]} - i\delta_{bc} X_{ad}^{[0]}, \end{aligned} \quad (69)$$

which is the $SU(4)$ [20]. The quantum Nambu algebra (67) is not exactly equivalent with the $SU(4)$ algebra (69), however, they have been treated almost synonymously thus far. This is because the known matrix realization of the fuzzy four-sphere was only the fully symmetric representation that satisfies both (67) and (69). The closed algebra (69) suggests that the natural symmetry in the lowest Landau level is the

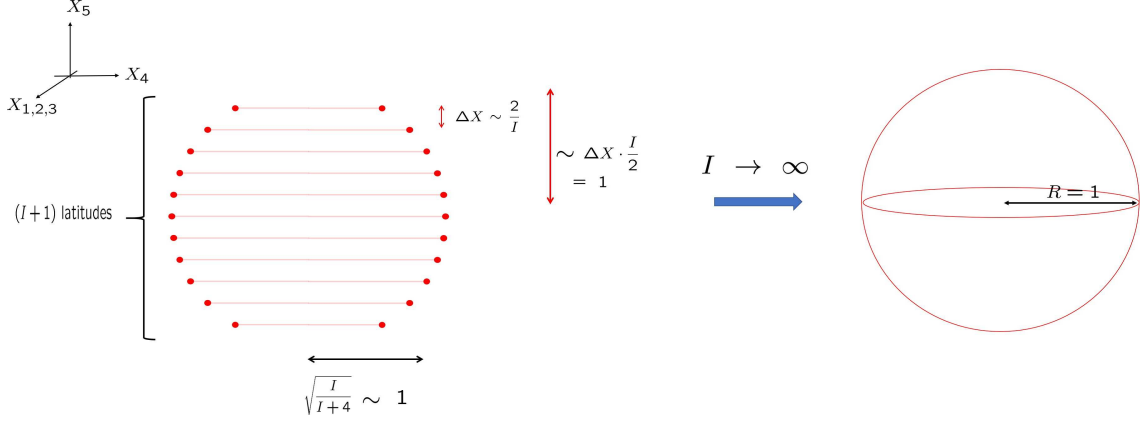


Figure 5: Fuzzy four-sphere in the lowest Landau level (the left) and its continuum limit (the right).

$SU(4)$ rather than the original $SO(5)$. This becomes clearer in the following discussion. The symmetric representation can be simply realized using the Schwinger boson operators.¹¹:

$$X_a^{[0]} = \frac{1}{I+4} \hat{\psi}_\alpha^\dagger (\gamma_a)_{\alpha\beta} \hat{\psi}_\beta \quad (70)$$

with

$$[\hat{\psi}_\alpha, \hat{\psi}_\beta^\dagger] = \delta_{\alpha\beta}, \quad [\hat{\psi}_\alpha, \hat{\psi}_\beta] = 0. \quad (71)$$

The boson number indicates the $SU(2)$ index of Yang's monopole :

$$\sum_{\alpha=1}^4 \hat{\psi}_\alpha^\dagger \hat{\psi}_\alpha = I. \quad (72)$$

One may readily check that (70) satisfy the $SU(4)$ algebra (69) together with $X_{ab}^{[0]} = -i\frac{1}{4}\hat{\psi}_\alpha^\dagger([\gamma_a, \gamma_b])_{\alpha\beta}\hat{\psi}_\beta$. The fuzzy manifold constructed from the $SU(4)$ matrices of the $SU(4)$ fully symmetric representation is referred to as the fuzzy \mathbb{CP}^3 [19]. Note that the dimension of the $SO(5)$ lowest Landau level $(p, q)_5 = (I, 0)_5$, is exactly equal to that of the $SU(4)$ fully symmetric representation:

$$D(0, I) = \frac{1}{3!}(I+1)(I+2)(I+3). \quad (73)$$

Therefore, the fuzzy S^4 is equivalent to the fuzzy \mathbb{CP}^3 (see Ref.[81] for discussions including matrix functions on them). The commutation relations of the Schwinger boson operators correspond to the canonical quantization of the homogeneous coordinates of the symplectic manifold \mathbb{CP}^3 . Therefore, it may be reasonable that the lowest Landau level geometry can be described within the conventional commutator formalism of the Lie algebra. The corresponding continuum limit is \mathbb{CP}^3 , which is the coset

$$\mathbb{CP}^3 \simeq SU(4)/U(3). \quad (74)$$

Here, we encounter the $SU(4)$ symmetry again. It is also worth noting that \mathbb{CP}^3 is locally equivalent to

$$\mathbb{CP}^3 \sim S^4 \times S^2. \quad (75)$$

While the original S^4 itself is not a symplectic manifold, the S^2 -fibre twisted on S^4 makes the entire bundle symplectic.

¹¹Historically, the Schwinger boson operators were utilized in the first construction of the fuzzy four-sphere [15]

4.2 Higher Landau level matrix geometry

From (50), we have

$$\text{tr}(X_5^{[N]^2}) = \frac{1}{(2N+I+4)^2(2N+I+2)^2} \sum_{n=0}^N (I+2+2n)^2 \sum_{s=-I/2}^{I/2} (2s)^2 d(n, I, s) = \frac{1}{5} c_1(N, I) D(N, I), \quad (76)$$

where

$$c_1(N, I) \equiv \frac{I(I+2)}{(2N+I+4)(2N+I+2)}. \quad (77)$$

Since all of $X_a^{[N]}$ are related by unitary transformations, their traces are the same, $\text{tr}(X_1^{[N]^2}) = \text{tr}(X_2^{[N]^2}) = \dots = \text{tr}(X_5^{[N]^2}) = \frac{1}{5} c_1 D$. The ortho-normal relation for $X_a[N]$ is given by

$$\text{tr}(X_a^{[N]} X_b^{[N]}) = \frac{1}{5} c_1(N, I) D(N, I) \delta_{ab}, \quad (78)$$

which implies Eq.(60):

$$\sum_{a=1}^5 X_a^{[N]} X_a^{[N]} = c_1(N, I) \mathbf{1}_{D(N, I)}. \quad (79)$$

One can explicitly check the validity of Eq.(79) using Eqs.(50) and (52). The radius of the fuzzy four-sphere is given by

$$R(N, I) \equiv \sqrt{c_1(N, I)} = \sqrt{\frac{I(I+2)}{(2N+I+4)(2N+I+2)}} \sim \frac{I}{2N+I}. \quad (80)$$

Since the matrix coordinates have two parameters, N and I , there are two different infinity limits of the radius:

$$\lim_{I \rightarrow \infty} R(N, I) = 1, \quad (81a)$$

$$\lim_{N \rightarrow \infty} R(N, I) = 0. \quad (81b)$$

Equation (81a) signifies the usual commutative limit in which the fuzzy four-sphere is reduced to the continuum four-sphere with a unit radius. On the other hand, Eq.(81b) indicates the collapse of the fuzzy four-spheres at $N \rightarrow \infty$. We will revisit this in Sec.4.3. It is demonstrated that $X_a^{[N]}$ satisfy the quantum Nambu algebra (61):

$$[X_a^{[N]}, X_b^{[N]}, X_c^{[N]}, X_d^{[N]}] = -4! c_3(N, I) \epsilon_{abcde} X_e^{[N]}, \quad (82)$$

where

$$c_3(N, I) \equiv -\frac{5}{c_1(N, I) D(N, I)} \text{tr}(X_1^{[N]} X_2^{[N]} X_3^{[N]} X_4^{[N]} X_5^{[N]}). \quad (83)$$

For instance, $\text{tr}(X_1^{[N]} X_2^{[N]} X_3^{[N]} X_4^{[N]} X_5^{[N]}) = -\frac{2896}{7503125}, -\frac{217}{124416}, -\frac{856}{5250987}$ for $(N, I) = (1, 1), (1, 2), (2, 1)$.¹² The matrix coordinates of the higher Landau levels not only satisfy the quantum Nambu algebra (82) but also encompass all possible matrix realizations of that algebra, because the higher Landau level matrix geometries encompass all possible irreducible representations of $SO(5)$.

¹²In the lowest Landau level, we have

$$\text{tr}(X_1^{[0]} X_2^{[0]} X_3^{[0]} X_4^{[0]} X_5^{[0]}) = \left(\frac{1}{I+4}\right)^5 \text{tr}(\Gamma_1 \Gamma_2 \Gamma_3 \Gamma_4 \Gamma_5) = -\frac{1}{90(I+4)^4} I(I+1)(I+2)^2(I+3), \quad (84)$$

and Eq.(82) reproduces Eq.(67).

It is also easy to see

$$[X_a^{[N]}, X_b^{[N]}] \not\propto i\Sigma_{ab}^{[N]} \quad (N \geq 1), \quad (85)$$

where $\Sigma_{ab}^{[N]}$ denote the $SO(5)$ generators in the $(N+I, I)_5$ representation. Equation (85) is consistent with the general discussions in Sec.2.3.2. While the commutators of X_a do not give rise to the $SO(5)$ generators, X_a themselves transform as an $SO(5)$ vector:

$$[X_a^{[N]}, \Sigma_{bc}^{[N]}] = -i\delta_{ab}X_c^{[N]} + i\delta_{ac}X_b^{[N]}. \quad (86)$$

The higher Landau level geometry is thus the one that adheres to the quantum Nambu algebra but *not* the $SU(4)$ algebra in contrast to the lowest Landau level matrix geometry. Let us recall again that the present scheme is beyond the conventional commutator formalism. The quantum geometry in the higher Landau levels is thus qualitatively different to that of the lowest Landau level. The algebraic structure of the higher Landau level geometry is apparent only after introducing the quantum Nambu bracket and cannot be captured by the ordinary commutator formalism. In this sense, the higher Landau level geometry is considered to be a *pure* quantum Nambu geometry.

4.3 Nested fuzzy four-sphere

Let us delve into the matrix structure of $X_a^{[N]}$. We represent (50) by the following $D(N, I) \times D(N, I)$ matrix (the upper left of Fig.6):

$$X_5^{[N]} = \bigoplus_{n=0}^N X_5^{(n)} = \begin{pmatrix} X_5^{(0)} & 0 & 0 & 0 & 0 \\ 0 & X_5^{(1)} & 0 & 0 & 0 \\ 0 & 0 & X_5^{(2)} & 0 & 0 \\ 0 & 0 & 0 & \ddots & 0 \\ 0 & 0 & 0 & 0 & X_5^{(N)} \end{pmatrix}, \quad (87)$$

where

$$\begin{aligned} X_5^{(n)} &= \frac{I+2n+2}{(2N+I+4)(2N+I+2)} \bigoplus_{s=-I/2}^{I/2} 2s \mathbf{1}_{d(n, I, s)} \\ &= \frac{I+2n+2}{(2N+I+4)(2N+I+2)} \begin{pmatrix} I\mathbf{1}_{d(n, I, I/2)} & 0 & 0 & 0 & 0 \\ 0 & (I-2)\mathbf{1}_{d(n, I, I/2-1)} & 0 & 0 & 0 \\ 0 & 0 & (I-4)\mathbf{1}_{d(n, I, I/2-2)} & 0 & 0 \\ 0 & 0 & 0 & \ddots & 0 \\ 0 & 0 & 0 & 0 & -I\mathbf{1}_{d(n, I, -I/2)} \end{pmatrix}. \end{aligned} \quad (88)$$

The diagonal blocks in $X_\mu^{[N]}$ that correspond to $X_5^{(n)}$ are denoted as $X_\mu^{(n)}$ (the lower right in Fig.6), which signify the matrix coordinates on the $SO(4)$ line (n) . We will delve into the matrix structure of $X_a^{(n)}$ that represents the fuzzy geometry on the $SO(4)$ line (n) . The sum of the squares of $X_a^{(n)}$ is given by

$$\sum_{a=1}^5 X_a^{(n)} X_a^{(n)} = \bigoplus_{s=-I/2}^{I/2} R^{(n, s)^2} \mathbf{1}_{d(n, I, s)} = \begin{pmatrix} R^{(n, I/2)^2} \mathbf{1}_{(n+I+1)(n+1)} & 0 & \cdots & 0 \\ 0 & R^{(n, I/2-1)^2} \mathbf{1}_{(n+I)(n+2)} & 0 & 0 \\ \vdots & 0 & \ddots & 0 \\ 0 & 0 & 0 & R^{(n, -I/2)^2} \mathbf{1}_{(n+1)(n+I+1)} \end{pmatrix}, \quad (89)$$

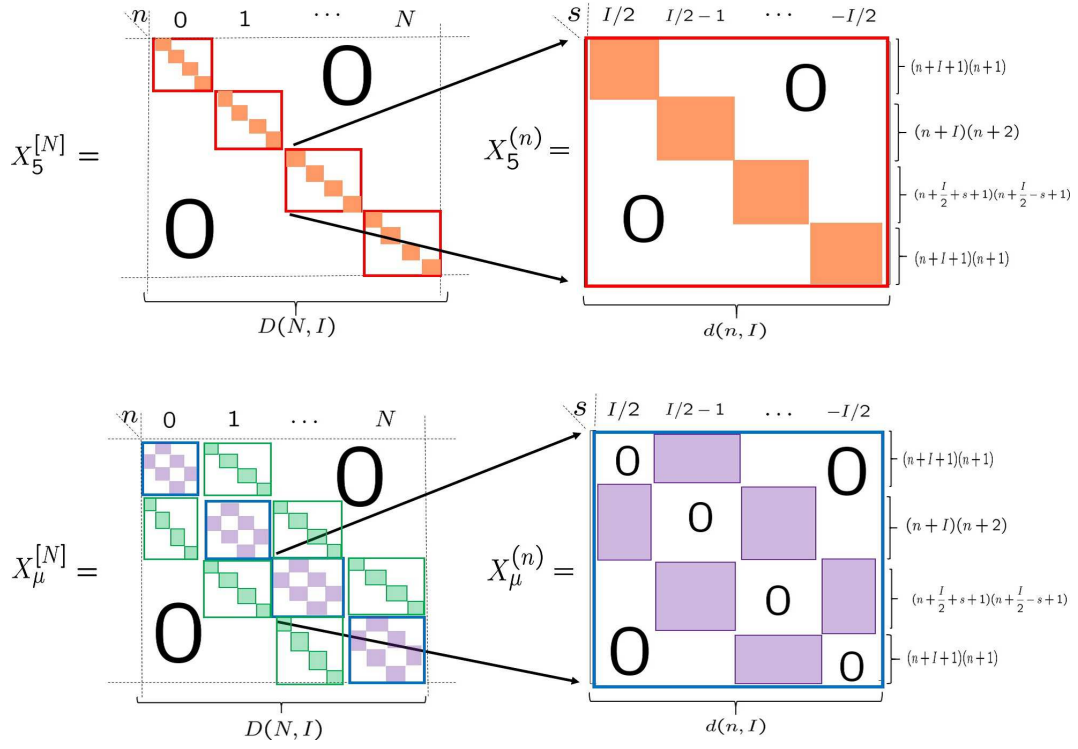


Figure 6: Matrix coordinates of the N th Landau level. Non-zero matrix elements are denoted as the shaded color regions.

where

$$R^{(n,s)} \equiv \frac{I + 2n + 2}{(2N + I + 4)(2N + I + 2)} \sqrt{2(B(j,k) + B(k,j)) + (2s)^2} = R^{(n,-s)} \quad (90)$$

with $B(j,k)$ defined by (104). Thus, $\sum_{a=1}^5 X_a^{(n)} X_a^{(n)}$ is not proportional to unit matrix $\mathbf{1}_{d(n,I)}$ (except for the special case $I = 1$)¹³, and so $X_a^{(n)}$ does *not* give rise to a complete fuzzy four-sphere geometry but provides a fuzzy four-sphere-like structure referred to as the quasi-fuzzy four-sphere [55]. The $I + 1$ diagonal blocks on the most right-hand side of Eq.(89) signify the $I + 1$ fuzzy hyper hyper-latitudes on the quasi-fuzzy four-sphere. Inside the matrix coordinates $X_a^{[N]}$ (Fig.6), there exist such $N + 1$ quasi-fuzzy four-spheres $X_a^{(n=0,1,2,\dots,N)}$. The non-zero off-diagonal blocks of the $X_\mu^{[N]}$ (the green filled rectangles in the lower left of Fig.6) are interpreted as the interactions between the adjacent quasi-fuzzy four-spheres.

The nested geometry of the $N + 1$ quasi-fuzzy four-spheres is depicted in Fig.7. One should *not* confuse

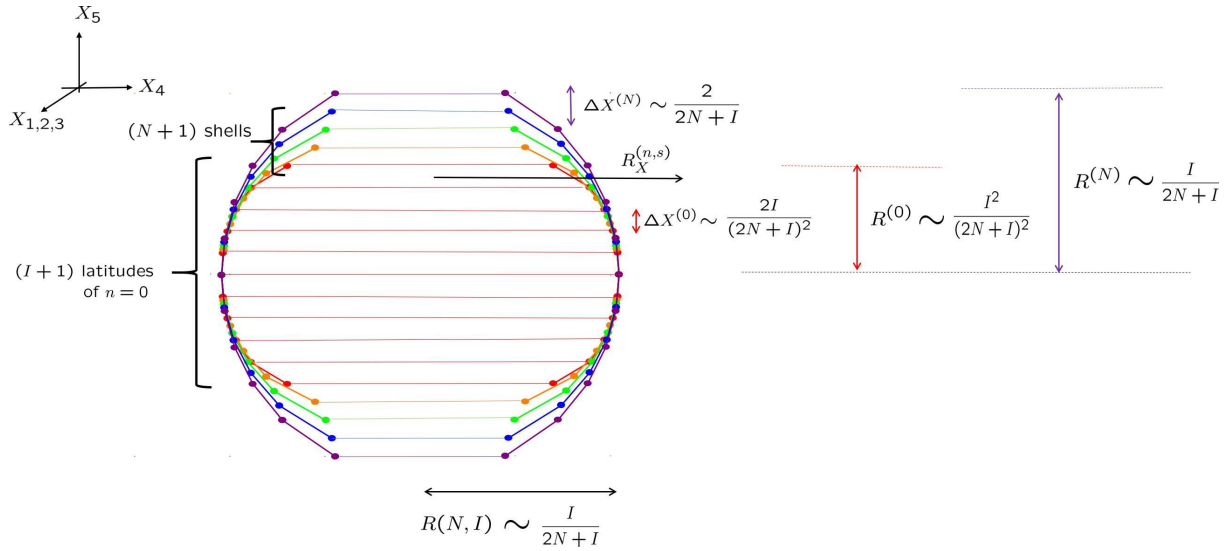


Figure 7: Matrix geometry of the N th higher Landau level is constituted from the $N + 1$ quasi-fuzzy four-spheres (and their interactions) to exhibit a nested fuzzy structure.

the present geometry with the nested structure made of a completely reducible representation [82]: In the case of the completely reducible representation, the nested fuzzy structure originates from the direct sum of the irreducible representations, while in the present, the nested fuzzy four-sphere is constituted from a single $SO(5)$ irreducible representation and each of the quasi-fuzzy four-spheres is not made of an $SO(5)$ irreducible representation (but rather consists of the $SO(4)$ representations on the $SO(4)$ line).¹⁴ Consequently, each quasi-fuzzy four-sphere is not regarded as an $SO(5)$ -symmetric object. This is also evident from the right-hand side of (89), which is apparently not $SO(5)$ invariant. The quasi-fuzzy four-spheres along with their interactions collectively form an $SO(5)$ -symmetric fuzzy manifold. We would like to draw the analogy to benzene. Each Kekulé structure only respects the C_3 rotational symmetry, while

¹³For $I = 1$, we have only two hyper-latitudes with the same radius, and $\sum_{a=1}^5 X_a^{(n)} X_a^{(n)}$ is proportional to $\mathbf{1}$:

$$\sum_{\mu=1}^a X_a^{(n)} X_a^{(n)} = \left(\frac{2n+3}{(2N+5)(2N+3)} \right)^2 \left(2 \frac{(N+2)^2}{(n+2)(n+1)} + 1 \right) \mathbf{1}_{2d(n,1)=2(n+2)(n+1)}. \quad (91)$$

¹⁴The very fuzzy fibres of fuzzy geometry is reported in [83, 84, 85]. That structure originates from the direct sum of irreducible representations, and so it is more akin to [82] than the present one. I would like to thank Harold Steinacker for valuable email communications on this point.

quantum mechanical superposition of two Kekulé structures results in benzene, which exhibits higher C_6 symmetry. Such a structure cannot be comprehended without quantum mechanics, and benzene realizes a purely quantum mechanical structure with no classical counterpart. In a similar sense, the nested fuzzy four-sphere can be considered a *pure* quantum geometry. This stems from the present quantum-oriented scheme, which can encompass pure quantum geometries.

The non-commutative scale differs in each of the quasi-fuzzy four-spheres (88):

$$\Delta X^{(n)} = \frac{2}{(2N + I + 4)(2N + I + 2)}(2n + I + 2), \quad (92)$$

and the “radius” of the quasi-fuzzy four-sphere is estimated as

$$R^{(n)} \sim \Delta X^{(n)} \cdot \frac{I}{2} = \frac{1}{(2N + I + 4)(2N + I + 2)}(2n + I + 2)(I + 1) \sim \frac{(2n + I)I}{(2N + I)^2}. \quad (93)$$

The outer quasi-fuzzy four-spheres have wider non-commutative scales (see Fig.7). It can be confirmed that the outermost quasi-fuzzy four-sphere of $n = N$ (93) exhibits the same behavior as the nested fuzzy four-sphere (80), as anticipated. We now provide an intuitive explanation for the previous result of the two limits (81). In the commutative limit $I \rightarrow \infty$, while $\Delta X^{(n)} \sim \frac{2}{I}$ (92) is reduced to zero, the number of the hyper-latitudes I goes to infinity. These two contributions are compensated to realize a continuum four-sphere with a unit radius, which simultaneously implies that all of the $N + 1$ quasi-fuzzy four-spheres are reduced to the single four-sphere.¹⁵ On the other hand, in the limit $N \rightarrow \infty$, while the number of hyper-latitudes remains unchanged, the non-commutative length (92) $\Delta X^{(n)} \sim \frac{1}{N}$ converges to zero. This leads to the collapse of the very nested fuzzy four-sphere, $R^{(n)} \rightarrow 0$ (Fig.8).

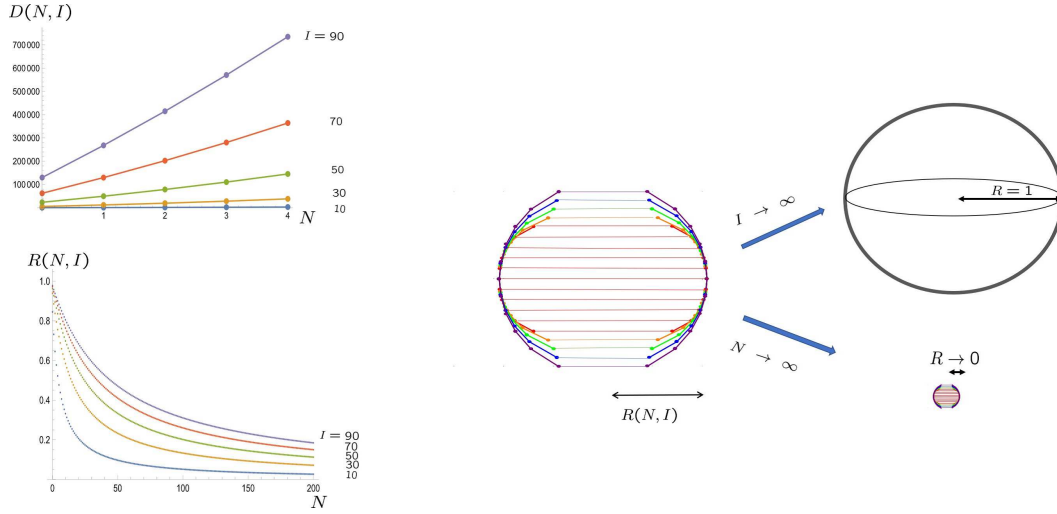


Figure 8: Behaviors of the quantities of the nested fuzzy four-sphere: The degeneracies (the upper left) and the radii (the lower left), the continuum limit $I \rightarrow \infty$ (the upper right) and the $N \rightarrow \infty$ limit (the lower right).

¹⁵In the commutative limit $I \rightarrow \infty$, each point on the four-sphere is highly degenerate. Because of the $SO(5)$ symmetry, we can count this degeneracy, for instance, at the north pole $X_5^{(n)} = 1$:

$$I \sum_{n=0}^N (n+1) = I \frac{1}{2} (N+1)(N+2). \quad (94)$$

5 Internal matrix geometry

Fuzzy three-sphere geometry can be realized as a sub-manifold of the (unnested) fuzzy four-sphere. Here, we explore the generalization of this concept for the nested fuzzy four-spheres.

5.1 Fuzzy hyper-latitudes

The quasi-fuzzy four-sphere is constituted from the $SO(4)$ irreducible representations on the $SO(4)$ line (n) . The matrix coordinates of the hyper-latitudes on the quasi-fuzzy four-sphere are readily derived from Eq.(56):

$$(Y_\mu^{(n)})_{m'_j, m'_k; m_j, m_k} \equiv \langle Y_{j', m'_j, k', m'_k} | y_\mu | Y_{j, m_j, k, m_k} \rangle \Big|_{j'+k'=j+k=n+\frac{I}{2}}, \quad (95)$$

which denotes a $d(n, I) \times d(n, I)$ matrix.¹⁶ The sum of the squares of $Y_\mu^{(n)}$ is given by

$$\sum_{\mu=1}^4 Y_\mu^{(n)} Y_\mu^{(n)} = \bigoplus_{s=-I/2}^{I/2} \mathcal{R}_Y^{(n,s)^2} \mathbf{1}_{d(n,I,s)} = \begin{pmatrix} \mathcal{R}_Y^{(n, \frac{I}{2})^2} \mathbf{1}_{(n+I+1)(n+1)} & 0 & \cdots & 0 \\ 0 & \mathcal{R}_Y^{(n, \frac{I}{2}-1)^2} \mathbf{1}_{(n+I)(n+2)} & 0 & 0 \\ 0 & 0 & \ddots & 0 \\ 0 & 0 & 0 & \mathcal{R}_Y^{(n, -\frac{I}{2})^2} \mathbf{1}_{(n+I+1)(n+1)} \end{pmatrix}, \quad (98)$$

where

$$\mathcal{R}_Y^{(n,s)} \equiv \sqrt{A(j, k) + A(k, j)} = \mathcal{R}_Y^{(n, -s)} \quad (99)$$

with

$$A(j, k) \equiv 2(j+1)k \left\{ \begin{matrix} j + \frac{1}{2} & k - \frac{1}{2} & \frac{I}{2} \\ k & j & \frac{1}{2} \end{matrix} \right\}^2. \quad (100)$$

Note $A(\frac{n}{2} + \frac{I}{2}, \frac{n}{2}) = 0$. Equation (98) represents a block diagonal matrix, with diagonal blocks indicating the hyper-latitudes of the radius $\mathcal{R}_Y^{(n,s)}$. At $I \rightarrow \infty$ and $|s| \ll I$, we have

$$\mathcal{R}_Y^{(n,s)} \rightarrow 1 \quad (A(j, k) \rightarrow \frac{1}{2}). \quad (101)$$

¹⁶The matrix $Y_\mu^{(n)}$ has the same matrix form as $X_\mu^{(n)}$ (the lower right of Fig.6):

$$Y_\mu^{(n)} = \begin{pmatrix} 0 & \mathcal{Y}_\mu^{(+-)}(\frac{I+n-1}{2}, \frac{n+1}{2}) & 0 & 0 & 0 & 0 \\ \mathcal{Y}_\mu^{(+-)}(\frac{I+n-1}{2}, \frac{n+1}{2})^\dagger & 0 & \mathcal{Y}_\mu^{(+-)}(\frac{I+n-2}{2}, \frac{n+2}{2}) & 0 & 0 & 0 \\ 0 & \mathcal{Y}_\mu^{(+-)}(\frac{I+n-2}{2}, \frac{n+2}{2})^\dagger & 0 & \mathcal{Y}_\mu^{(+-)}(\frac{I+n-3}{2}, \frac{n+3}{2}) & 0 & 0 \\ 0 & 0 & \mathcal{Y}_\mu^{(+-)}(\frac{I+n-3}{2}, \frac{n+3}{2})^\dagger & 0 & \ddots & 0 \\ 0 & 0 & 0 & \ddots & 0 & \mathcal{Y}_\mu^{(+-)}(\frac{n}{2}, \frac{n+I}{2}) \\ 0 & 0 & 0 & 0 & \mathcal{Y}_\mu^{(+-)}(\frac{n}{2}, \frac{n+I}{2})^\dagger & 0 \end{pmatrix}, \quad (96)$$

and $A(j, k)$ and $A(k, j)$ in (99) are given by

$$\sum_{\mu=1}^4 \mathcal{Y}_\mu^{(+-)}(j, k)^\dagger \mathcal{Y}_\mu^{(+-)}(j, k) = A(j, k) \mathbf{1}_{(2j+1)(2k+1)}, \quad (97a)$$

$$\sum_{\mu=1}^4 \mathcal{Y}_\mu^{(+-)}(j - \frac{1}{2}, k + \frac{1}{2}) \mathcal{Y}_\mu^{(+-)}(j - \frac{1}{2}, k + \frac{1}{2})^\dagger = A(k, j) \mathbf{1}_{(2j+1)(2k+1)}. \quad (97b)$$

Around $s \sim 0$, the radii of the hyper-latitudes converge to unity, as anticipated from $\sum_{\mu=1}^4 y_\mu y_\mu = 1$. The hyper-latitudes for s as the vertical axis are depicted in the left of Fig. 9.

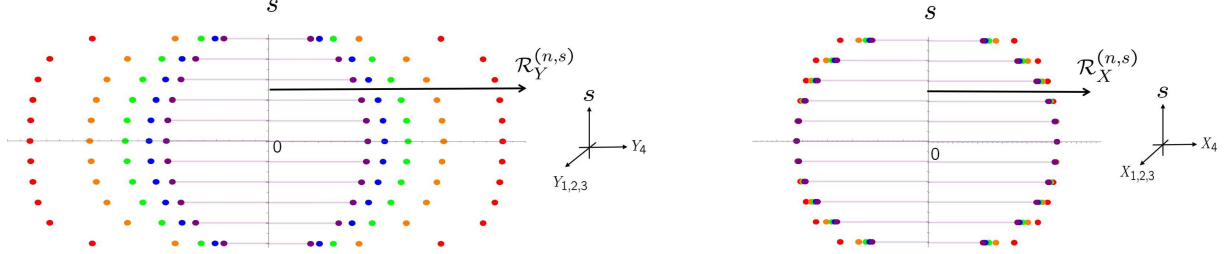


Figure 9: The distributions of $\mathcal{R}_Y^{(n,s)}$ (the left) and $\mathcal{R}_X^{(n,s)}$ (the right) for $I/2 = 5$. The $SO(4)$ line index $n(= 0, 1, 2, 3, 4)$ corresponds to red, orange, green, blue and purple points, respectively.

We also evaluate the radii of the hyper-latitudes within the quasi-fuzzy four-sphere. Using Eq.(52), we can derive

$$\sum_{\mu=1}^4 X_\mu^{(n)} X_\mu^{(n)} = \bigoplus_{s=-I/2}^{I/2} \mathcal{R}_X^{(n,s)^2} \mathbf{1}_{d(n,I,s)} = \begin{pmatrix} \mathcal{R}_X^{(n,\frac{I}{2})^2} \mathbf{1}_{(n+I+1)(n+1)} & 0 & \cdots & 0 \\ 0 & \mathcal{R}_X^{(n,\frac{I}{2}-1)^2} \mathbf{1}_{(n+I)(n+2)} & 0 & 0 \\ 0 & 0 & \ddots & 0 \\ 0 & 0 & 0 & \mathcal{R}_X^{(n,-\frac{I}{2})^2} \mathbf{1}_{(n+I+1)(n+1)} \end{pmatrix}, \quad (102)$$

where

$$\mathcal{R}_X^{(n,s)} \equiv \frac{2n + I + 2}{(2N + I + 2)(2N + I + 4)} \sqrt{B(j,k) + B(k,j)} = \mathcal{R}_X^{(n,-s)}, \quad (103)$$

with

$$B(j,k) \equiv 4 \left(N + \frac{I}{2} - j + k + 1 \right) \left(N + \frac{I}{2} + j - k + 2 \right) A(j,k). \quad (104)$$

For the distributions of $\mathcal{R}_X^{(n,\frac{I}{2})}$, see the right of Fig.9. Obviously, the distribution of points of the same color forms a quasi-fuzzy four-sphere. (The distribution of $\mathcal{R}_X^{(n,s)}$ is illustrated in Fig. 7 with X_5 as the vertical axis.) At $I \rightarrow \infty$ and $|s| \ll I$, we have

$$\mathcal{R}_X^{(n,s)} \rightarrow 1 \quad (B(j,k) \rightarrow \frac{1}{2} I^2). \quad (105)$$

When I is even, $\mathcal{R}_X^{(n,s)}$ takes the maximum value at $s = j - k = 0$:

$$\mathcal{R}_X^{(n,s=0)} = \sqrt{\frac{I(I+2)}{(2N+I+4)(2N+I+2)}}. \quad (106)$$

This quantity does not depend on n , indicating that the equators of all the quasi-fuzzy four-spheres have the same radius, which is identical to the radius of the fuzzy S^4 (80) (see Fig.7 also).

5.2 Fuzzy three-sphere

The fuzzy three-sphere is naturally embedded within the geometry of the fuzzy four-sphere [18, 21, 23]. This sub-space is composed of $SO(4)$ representations with $s = 1/2 \oplus -1/2$. In the case of the usual

(un-nested) fuzzy four-sphere, there exists only one fuzzy three-sphere around the equator of the fuzzy four-sphere. In contrast, the nested fuzzy four-sphere consists of multiple quasi-fuzzy four-spheres, each of which accommodates a fuzzy three-sphere. Consequently, the N th Landau level fuzzy four-sphere hosts $N + 1$ fuzzy three spheres around its equator. To extract the fuzzy three-sphere geometry, we focus on the $s = 1/2 \oplus -1/2$ sub-space of the matrix coordinates $Y_\mu^{(n)}$. For odd integer I , we can derive the fuzzy three-sphere matrix coordinates (see Fig.10)

$$\mathbb{Y}_\mu^{(n)} = \begin{pmatrix} 0 & \mathcal{Y}_\mu^{(+)}(\frac{n}{2} + \frac{I}{4} - \frac{1}{4}, \frac{n}{2} + \frac{I}{4} + \frac{1}{4}) \\ \mathcal{Y}_\mu^{(-)}(\frac{n}{2} + \frac{I}{4} - \frac{1}{4}, \frac{n}{2} + \frac{I}{4} + \frac{1}{4})^\dagger & 0 \end{pmatrix}, \quad (107)$$

which satisfy

$$\sum_{\mu=1}^4 \mathbb{Y}_\mu^{(n)} \mathbb{Y}_\mu^{(n)} = R_\mathbb{Y}^{(n)2} \mathbf{1}_{2d(n, I, 1/2)} \quad (108)$$

where

$$R_\mathbb{Y}^{(n)} \equiv \sqrt{A(j, k)}|_{j=\frac{n}{2}+\frac{I}{4}-\frac{1}{4}, k=\frac{n}{2}+\frac{I}{4}+\frac{1}{4}} = \frac{I+1}{\sqrt{2(2n+I+1)(2n+I+3)}}. \quad (109)$$

Unlike the sum of the squares of $Y_\mu^{(n)}$ (98), Eq.(108) is proportional to a unit matrix. This implies that

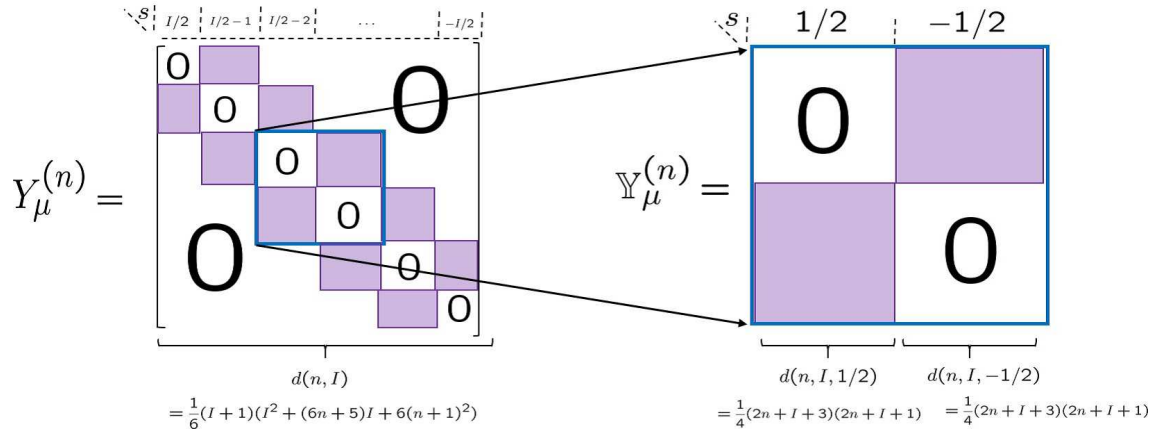


Figure 10: The fuzzy three-sphere matrix coordinates $\mathbb{Y}_\mu^{(n)}$ from $Y_\mu^{(n)}$ for odd I .

while $Y_\mu^{(n)}$ themselves cannot be regarded as the coordinates of the fuzzy three-sphere, their sub-block matrices $\mathbb{Y}_\mu^{(n)}$ can be. Furthermore, $\mathbb{Y}_\mu^{(n)}$ are shown to satisfy

$$[\mathbb{Y}_\mu^{(n)}, \mathbb{Y}_\nu^{(n)}, \mathbb{Y}_\rho^{(n)}] = 8(2n+I+2) \left(\frac{I+1}{(2n+I+1)(2n+I+3)} \right)^2 \epsilon_{\mu\nu\rho\sigma} \mathbb{Y}_\sigma^{(n)}, \quad (110)$$

where the “three bracket” $[\mathbb{Y}_\mu, \mathbb{Y}_\nu, \mathbb{Y}_\rho]$ is defined as

$$[\mathbb{Y}_\mu^{(n)}, \mathbb{Y}_\nu^{(n)}, \mathbb{Y}_\rho^{(n)}] \equiv [\mathbb{Y}_\mu^{(n)}, \mathbb{Y}_\nu^{(n)}, \mathbb{Y}_\rho^{(n)}, \Gamma_5] \quad (111)$$

with

$$\Gamma_5 \equiv \begin{pmatrix} \mathbf{1}_{d(n, I, 1/2)} & 0 \\ 0 & -\mathbf{1}_{d(n, I, -1/2)} \end{pmatrix}. \quad (112)$$

Equations (108) and (110) clearly show that $\mathbb{Y}_\mu^{(n)}$ realize the matrix coordinates of the fuzzy three-sphere.¹⁷ Fig.11 illustrates the behaviors of the matrix sizes and the radii (109) of fuzzy three-spheres. The qualitative

¹⁷With

$$\mathbb{Y}_5^{(n)} \equiv \frac{I+1}{2} \frac{1}{\sqrt{2(2n+I+3)(2n+I+1)}} \Gamma_5, \quad (113)$$

features of these quantities are similar to those of the fuzzy four-sphere (Fig.8) as the fuzzy three-spheres being embedded in of the fuzzy four-sphere. Note that the radius of the fuzzy three-sphere is not equal to that of the fuzzy hyper-latitude of the same s (99), $\mathcal{R}_Y^{(n,s=1/2)} \neq R_Y^{(n)}$, and $R_Y^{(n)}$ does not converge to unity in the continuum limit, $R_Y^{(n)} \xrightarrow{I \rightarrow \infty} 1/\sqrt{2} \neq 1$.

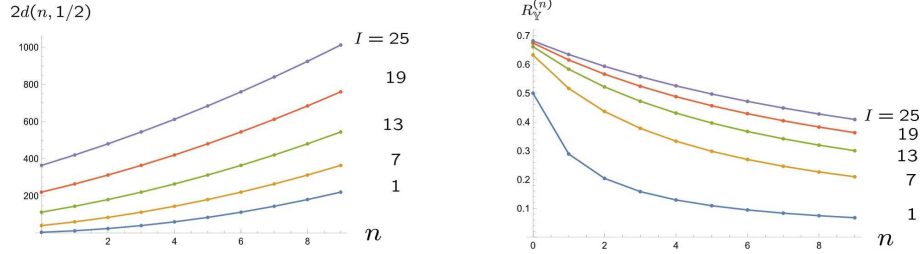


Figure 11: The matrix size and the radius of the fuzzy three-sphere.

We also explain how the fuzzy three-sphere itself is obtained within the present non-commutative framework, without referring to the geometry of the fuzzy four-sphere. Since S^3 can be identified with $SO(4)/SO(3)$, the stabilizer group $SO(3)$ is interpreted as the $SU(2)$ gauge symmetry on the quantum mechanics side. Then, we consider an $SU(2)$ gauged quantum mechanics on S^3 , known as the $SO(4)$ Landau model [54, 50, 46]. In this model, n represents the Landau level index, and s signifies the subband index. The $SO(4)$ Landau model exhibits degeneracy due to the presence of the left-right \mathbb{Z}_2 symmetry, in addition to the global $SO(4)$ symmetry. The fuzzy three-sphere geometry $\mathbb{Y}_\mu^{(n)}$ emerges in the lowest energy sub-bands with indices $s = 1/2, -1/2$, for arbitrary n th Landau level. The degenerate energy eigenstates that constitute the fuzzy three-sphere consist of the direct sum of irreducible representations of the global symmetry $SO(4)$, which is an irreducible representation of the entire symmetry group $SO(4) \otimes \mathbb{Z}_2$.

6 Continuum limit and the S^4 geometry

We discuss the continuum limit and the classical geometry of the nested fuzzy four-sphere. While the continuum limit of the fuzzy two-sphere is the usual classical two-sphere, this is not generally the case for other fuzzy manifolds. For instance, the continuum limit of the unnested fuzzy $2k$ -sphere yields the symplectic manifold $SO(2k+1)/U(k)$ [20], which is obviously distinct from S^{2k} .

6.1 The 2nd Hopf map

The Hopf maps are a key to bridge non-commutative geometry and classical geometry [39]. The second Hopf map

$$\psi_{\alpha=1,2,3,4} (\psi_\alpha^* \psi_\alpha = 1) \in S^7 \rightarrow x_a = \psi_\alpha^* (\gamma_a)_{\alpha\beta} \psi_\beta \in S^4 \quad (x_a x_a = (\psi_\alpha^\dagger \psi_\alpha)^2 = 1) \quad (116)$$

$\mathbb{Y}_{\mu=1,2,3,4}^{(n)}$ satisfy the orthonormal condition:

$$\text{tr}(\mathbb{Y}_a^{(n)} \mathbb{Y}_b^{(n)}) = \left(\frac{I+1}{4} \right)^2 \delta_{ab}. \quad (114)$$

Equation (110) is realized as a special case of the four-algebra,

$$[\mathbb{Y}_a^{(n)}, \mathbb{Y}_b^{(n)}, \mathbb{Y}_c^{(n)}, \mathbb{Y}_d^{(n)}] = -2\sqrt{2} (I+1)^3 \frac{2n+I+2}{\sqrt{(2n+I+3)(2n+I+1)^5}} \epsilon_{abcde} \mathbb{Y}_e^{(n)}. \quad (115)$$

provides a clear understanding of the fuzzy four-sphere geometry. The fuzzification is simply executed by replacing the components of the Hopf spinor with four annihilation operators:

$$\psi_\alpha \rightarrow \frac{1}{\sqrt{I+4}} \hat{\psi}_\alpha, \quad (117)$$

with

$$[\hat{\psi}_\alpha, \hat{\psi}_\beta^\dagger] = \delta_{\alpha\beta}, \quad [\hat{\psi}_\alpha, \hat{\psi}_\beta] = 0. \quad (118)$$

The “quantized” Hopf map is now given by

$$\hat{\psi}_\alpha \quad (\hat{\psi}_\alpha^\dagger \hat{\psi}_\alpha = I) \rightarrow X_a = \frac{1}{I+4} \hat{\psi}_\alpha^\dagger (\gamma_a)_{\alpha\beta} \hat{\psi}_\beta, \quad (119)$$

which satisfy

$$X_a X_a = \frac{1}{(I+4)^2} (\hat{\psi}_\alpha^\dagger \hat{\psi}_\alpha) (\hat{\psi}_\beta^\dagger \hat{\psi}_\beta + 4) = \frac{I}{I+4}. \quad (120)$$

Notice that X_a (119) coincide with the lowest Landau level coordinate operators (70). The total manifold S^7 represents the classical manifold of the Hopf spinor and the S^7 modulo $U(1)$ phase is $\mathbb{C}P^3$, which is the continuum limit of the (unnested) fuzzy four-sphere. The second Hopf map thus presents a relationship between the unnested fuzzy four-sphere and its continuum limit.

Also notice that the Hopf spinor for (116) can be chosen as

$$\psi = \frac{1}{\sqrt{2(1+x_5)}} \begin{pmatrix} 1+x_5 \\ 0 \\ x_4 - ix_3 \\ x_2 - ix_1 \end{pmatrix} = \begin{pmatrix} \cos \frac{\xi}{2} \\ 0 \\ \sin \frac{\xi}{2} (\cos \chi - i \sin \chi \cos \theta) \\ -i \sin \frac{\xi}{2} \sin \chi \sin \theta e^{i\phi} \end{pmatrix}, \quad (121)$$

which satisfies

$$\sum_{a=1}^5 x_a \gamma_a \psi = +\psi. \quad (122)$$

This is the simplest version of the $SO(5)$ spin-coherent state equation, which plays a central role in deriving the classical geometry of the fuzzy four-sphere in Sec.6.3.1.

6.2 Continuum limit

To expand a concrete discussion, let us focus on the north point of the nested fuzzy four-sphere. Since the nested fuzzy four-sphere is an $SO(5)$ symmetric object, we can choose the north pole as a reference point without loss of generality. The north pole is represented by the index $s = I/2$, which correspond to the $N+1$ most right edges of the oblique $SO(4)$ lines in Fig.3:

$$\bigoplus_{n=0}^N (j, k)|_{s=I/2} = \bigoplus_{n=0}^N \left(\frac{I}{2} + \frac{n}{2}, \frac{n}{2} \right)_4. \quad (123)$$

Since j and k are two independent $SU(2)$ indices, the $(j, k)_4$ realizes a direct product of two fuzzy spheres specified by the $SU(2)$ spins, j and k , in the language of the fuzzy geometry. In the continuum limit $I \rightarrow \infty$, Eq.(123) becomes

$$\bigoplus_{n=0}^N (j, k)|_{s=I/2} \sim \bigoplus_{n=0}^N \left(\frac{I}{2}, 0 \right), \quad (124)$$

which suggests that the fuzzy structure of the north pole is well approximated by the $N+1$ identical fuzzy two-spheres, each with the $SU(2)$ spin $I/2$. Since every $SO(4)$ line or quasi-fuzzy four-sphere thus

accommodates a fuzzy two-sphere, each quasi-fuzzy four-sphere is described locally by $S^4 \times S^2$, or \mathbb{CP}^3 in the continuum. Consequently, the nested fuzzy four-sphere is reduced to $N + 1$ overlapped identical \mathbb{CP}^3 s. This is also suggested by the continuum limit of the degeneracy (45)

$$D(N, I) \xrightarrow{I \rightarrow \infty} (N + 1) \cdot \frac{1}{6} I^3, \quad (125)$$

where $\frac{1}{6} I^3$ denotes the degrees of freedom of a single fuzzy \mathbb{CP}^3 .

It should be emphasized that while the continuum limit of the nested fuzzy four-sphere is $N + 1$ overlapped \mathbb{CP}^3 s, their fuzzification does not recover the original nested fuzzy four-sphere but just provides $N + 1$ identical fuzzy \mathbb{CP}^3 s (or $N + 1$ unnested identical fuzzy four-spheres). In other words, the nested fuzzy four-sphere geometry cannot be reproduced from its corresponding continuum manifold. This agrees with the previous observation that the nested fuzzy four-sphere is a pure quantum object.

6.3 S^4 geometry

The coherent state method [88, 89, 90] and the probe brane method [91, 92, 93] are systematic methods to obtain a classical manifold corresponding to a given matrix geometry. These two methods are related but not exactly the same [60, 93]. Here, we derive the S^4 geometry from the matrix coordinates using there methods.

6.3.1 Coherent state method

For matrix coordinates X_a , the coherent method [88, 89, 90] adopts the following matrix Hamiltonian,

$$H = \sum_{a=1}^5 (X_a^{[N]} - x_a \mathbf{1}_{D(N, I)})^2. \quad (126)$$

We can derive classical manifold as a configuration of x_a by following the three steps: First, we diagonalize the matrix Hamiltonian to derive the groundstate energy $E_G(x_a)$. Second, we examine the minimum of $E_G(x_a)$ as a function of x_a to determine the vacuum manifold of x_a . Last, we take the $I \rightarrow \infty$ limit of this configuration.

The matrix Hamiltonian (126) is rewritten as

$$H = X_a^{[N]2} - 2x_a X_a^{[N]} + r^2 \mathbf{1}_{D(N, I)} = \left(\frac{I(I+2)}{(2N+I+4)(2N+I+2)} + r^2 \right) \mathbf{1}_{D(N, I)} - 2x_a X_a^{[N]}, \quad (127)$$

with

$$r \equiv \sqrt{x_a x_a}. \quad (128)$$

The cross term of Eq.(127) is diagonalized as

$$U(\xi, \chi, \theta, \phi)^\dagger (x_a X_a^{[N]}) U(\xi, \chi, \theta, \phi) = r X_5^{[N]}, \quad (129)$$

where

$$U(\xi, \chi, \theta, \phi) \equiv H(\chi, \theta, \phi)^\dagger e^{i\xi \Sigma_{45}^{[N]}} H(\chi, \theta, \phi) \quad (H(\chi, \theta, \phi) \equiv e^{-i\chi \Sigma_{34}^{[N]}} e^{i\theta \Sigma_{31}^{[N]}} e^{i\phi \Sigma_{12}^{[N]}}). \quad (130)$$

The maximal eigenvalue of $X_5^{[N]}$ is attained at the north pole $s = I/2$ of the outermost quasi-fuzzy four-sphere $n = N$ with degeneracy $d(N, I, s = I/2)$:

$$X_5^{[N]} e_\sigma = \frac{I}{2N+I+4} e_\sigma \quad (\sigma = 1, 2, \dots, d(N, I, I/2)). \quad (131)$$

Here, \mathbf{e}_σ denotes a $D(N, I)$ -component unit vector with $(\mathbf{e}_\sigma)_{\alpha=1,2,\dots,D(N,I)} \equiv \delta_{\sigma\alpha}$. The $SO(5)$ rotation of \mathbf{e}_σ to align with the direction of x_a will result in

$$(x_a X_a^{[N]}) \Psi_\sigma^{[N,I]} = r \frac{I}{2N + I + 4} \Psi_\sigma^{[N,I]}, \quad (132)$$

where

$$\Psi_\sigma^{[N,I]}(\xi, \chi, \theta, \phi) \equiv U(\xi, \chi, \theta, \phi) \mathbf{e}_\sigma = \begin{pmatrix} U_{1,\sigma} \\ U_{2,\sigma} \\ \vdots \\ U_{D,\sigma} \end{pmatrix}. \quad (133)$$

Equation (132) signifies a generalized $SO(5)$ spin-coherent state equation and its simplest version ($N = 0, I = 1$) corresponds to Eq.(122).¹⁸ The spin-coherent states (133) constitute an ortho-normal set:¹⁹

$$\Psi_\sigma^{[N,I]}(\xi, \chi, \theta, \phi)^\dagger \Psi_\tau^{[N,I]}(\xi, \chi, \theta, \phi) = \delta_{\sigma\tau}. \quad (135)$$

The ground state energy is then obtained as

$$E_G(r) = r^2 - 2r \frac{I}{2N + I + 4} + \frac{I(I + 2)}{(2N + I + 4)(2N + I + 2)}, \quad (136)$$

and the corresponding eigenstates are given by (133) with degeneracy

$$d(N, I, I/2) = (N + 1)(N + I + 1). \quad (137)$$

The classical vacuum of $E_G(r)$ (136) is attained by

$$r = \frac{I}{2N + I + 4}. \quad (138)$$

Note that Eq.(138) is equal to the radius of the outermost quasi-fuzzy four-sphere $n = N$ (93). From (138), we have

$$\lim_{I \rightarrow \infty} r = 1. \quad (139)$$

We thus obtained the classical S^4 geometry ($x_a x_a = 1$) from $X_a^{[N]}$.

6.3.2 Probe brane method

The probe brane method [91, 92, 93] adopts the Dirac-operator matrix

$$D(x_a) = \sum_{a=1}^5 \gamma_a \otimes (X_a^{[N]} - x_a \mathbf{1}_{D(N,I)}). \quad (140)$$

In this method, the classical manifold is obtained through the following two steps. First, we consider the condition for the existence of the zero-modes of the Dirac-operator matrix (140). For zero-modes to exist, x_a must satisfy a certain condition which characterizes a classical manifold. Subsequently, we take $I \rightarrow \infty$ limit of the classical manifold to derive the corresponding classical geometry. Due to the tensor product

¹⁸From (132), we have

$$\Psi_\sigma^{[N,I]\dagger} X_a^{[N]} \Psi_\sigma^{[N,I]} = r \frac{I}{2N + I + 4} x_a. \quad (134)$$

This concise form of the transformation from matrix coordinates X_a to classical coordinates x_a is given in Ref.[62].

¹⁹The $SO(5)$ spin-coherent states are closely related to the $SO(5)$ Landau level eigenstates (35), as both are realized in the unitary matrix (130) [57]. See Ref.[94] for more details.

form of (140), it is rather technically intricate to derive general results unlike the case of the coherent state method. Hence, we conduct numerical investigations by employing the explicit forms of $X_a^{[N]}$. The obtained numerical results imply

$$\det(D(x_a))|_{x_a x_a = (\frac{I}{2N+I+4})^2} = 0 \quad (141)$$

and the number of the zero-modes

$$d(N, I+1, (I+1)/2) = (N+1)(N+I+2). \quad (142)$$

Equation (141) indicates that the zero-modes exist when x_a satisfy $r = \frac{I}{2N+I+4}$, which is equal to the previous result (138). Therefore, both the coherent state method and the probe brane method yield the identical classical geometry in the present case. Meanwhile, the number of the zero-modes (142) is distinct from that of the coherent states (137).

7 Realization in Yang-Mills matrix models

In this section, we demonstrate that the nested fuzzy four-spheres realize new classical solutions of Yang-Mills matrix models and investigate their physical properties. In particular, we clarify distinct behaviors between the lowest Landau level matrix geometry and the newly obtained higher Landau level matrix geometries.

7.1 Basic relations

Using the explicit forms of $X_a^{[N]}$, we can demonstrate that $X_a^{[N]}$ satisfy

$$X_a^{[N]} X_a^{[N]} = c_1(N, I) \mathbf{1}_{D(N, I)}, \quad (143a)$$

$$X_b^{[N]} X_a^{[N]} X_b^{[N]} = c_2(N, I) X_a^{[N]}, \quad (143b)$$

$$\epsilon_{abcde} X_b^{[N]} X_c^{[N]} X_d^{[N]} X_e^{[N]} = -4! c_3(N, I) X_a^{[N]}, \quad (143c)$$

where c_1 and c_3 are given by (77) and (83), respectively. In principle, we can determine all of values of the c_s through Eq.(143). For instance, $c_2(1, 1) = -\frac{47}{1225}$, $c_2(1, 2) = \frac{5}{72}$, $c_2(1, 3) = \frac{211}{1323}$, $c_3(1, 1) = \frac{181}{128625}$, $c_3(1, 2) = \frac{31}{20736}$, $c_3(1, 3) = \frac{367}{250047}$.²⁰ Equations (143a) and (143b) imply

$$-\frac{1}{4}([X_a^{[N]}, X_b^{[N]}]^2) = \frac{1}{2}(c_1 - c_2)c_1 \mathbf{1}_{D(N, I)} \quad (145)$$

and the potential energy is expressed as

$$V(X_a^{[N]}) \equiv -\frac{1}{4}\text{tr}([X_a^{[N]}, X_b^{[N]}]^2) = \frac{1}{2}(c_1 - c_2)c_1 D(N, I). \quad (146)$$

The behaviors of the c_s and the V are illustrated in Fig.12. Their behaviors are similar to those of the fuzzy two-sphere (see Fig.16).

While we have utilized $X_a^{[N]}$ as the matrix coordinates, from an algebraic standpoint, it might be more natural to adopt "normalized" matrix coordinates that align with the quantum Nambu algebra:

$$[\hat{X}_a^{[N]}, \hat{X}_b^{[N]}, \hat{X}_c^{[N]}, \hat{X}_d^{[N]}] = -4!\epsilon_{abcde} \hat{X}_e^{[N]}, \quad (147)$$

²⁰In the lowest Landau level ($N = 0$), the coefficients are given by

$$c_1(0, I) = \frac{I}{I+4}, \quad c_2(0, I) = \frac{I^2 + 4I - 8}{(I+4)^2}, \quad c_3(0, I) = \frac{I+2}{3(I+4)^3}. \quad (144)$$

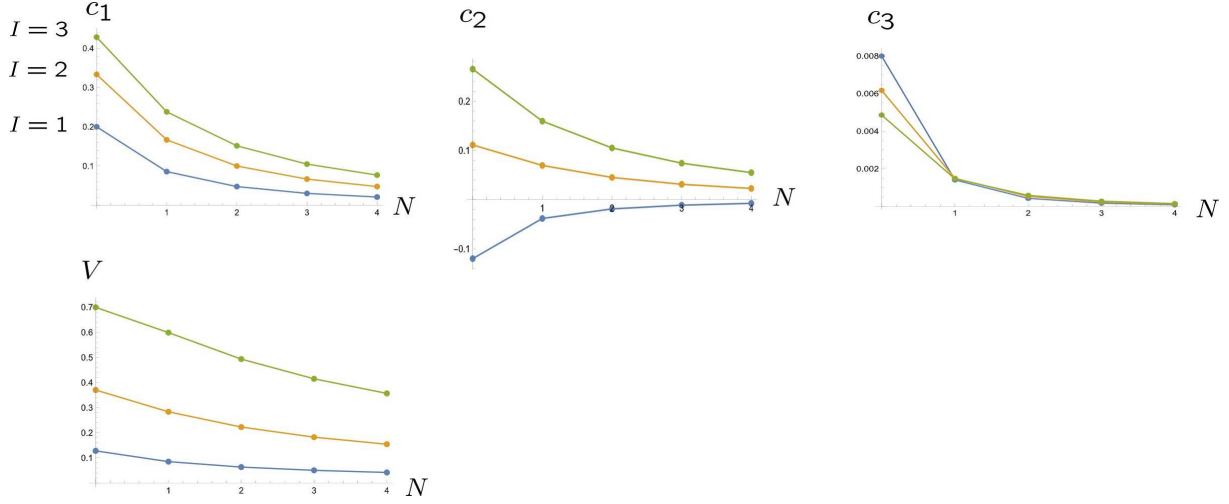


Figure 12: The upper: The behaviors of c_s . The blue, orange and green lines correspond to $I = 1, 2, 3$, respectively. The lower: the behaviors of the potential (146).

or

$$\hat{X}_a^{[N]} = \frac{1}{c_3^{1/3}} X_a^{[N]}. \quad (148)$$

For $\hat{X}_a^{[N]}$, important physical quantities are given by²¹

$$\text{radius} : \hat{R} \equiv \frac{c_1^{1/2}}{c_3^{1/3}} \quad (\hat{X}_a^{[N]} \hat{X}_a^{[N]} = \hat{R}^2 \mathbf{1}_{D(N,I)}), \quad (150a)$$

$$\text{potential energy} : \hat{V} = -\frac{1}{4} \text{tr}([\hat{X}_a^{[N]}, \hat{X}_b^{[N]}]^2) = \frac{1}{2c_3^{4/3}} (c_1 - c_2) c_1 D(N, I), \quad (150b)$$

$$\text{potential energy density} : \frac{\hat{V}}{\hat{R}^4} = -\frac{1}{4} \text{tr}([\hat{X}_a^{[N]}, \hat{X}_b^{[N]}]^2) = \frac{c_1 - c_2}{2c_1} D(N, I). \quad (150c)$$

The quantities in Eq.(150) are plotted in Fig.13. The radius \hat{R} increases as N increases (Fig.13) unlike the original R (80) (Fig.8). The behaviors of the quantities in Eq.(150) are qualitative similar to those of the fuzzy two-sphere (Fig.17), except for the potential energy densities (the lower right of Fig.13) in which the order of magnitudes for $I = 1, 2, 3$ is reversed between the lowest Landau level ($N = 0$) and the higher Landau levels ($N \geq 1$).

7.2 As classical solutions of Yang-Mills matrix models

7.2.1 With a mass term

Let us consider Yang-Mills matrix model with a mass term [95]:

$$S_{\text{mass}} = -\frac{1}{4} \text{tr}([A_a, A_b]^2) - \frac{1}{2} \rho \text{tr}(A_a^2) \quad (\rho > 0). \quad (151)$$

²¹In the lowest Landau level ($N = 0$), Eq.(148) is reduced to $\hat{X}_a^{[0]} = (\frac{3}{I+2})^{\frac{1}{3}} (I+4) X_a^{[0]} = (\frac{3}{I+2})^{\frac{1}{3}} \Gamma_a$, and Eq.(150) becomes

$$\hat{R} = I^{1/2} (I+4)^{1/2} \left(\frac{3}{I+2} \right)^{1/3}, \quad \hat{V} = 2 \left(\frac{3}{I+2} \right)^{1/3} I(I+1)(I+3)(I+4), \quad \frac{\hat{V}}{\hat{R}^4} = \frac{2}{3} \frac{(I+1)(I+2)(I+3)}{I(I+4)}. \quad (149)$$

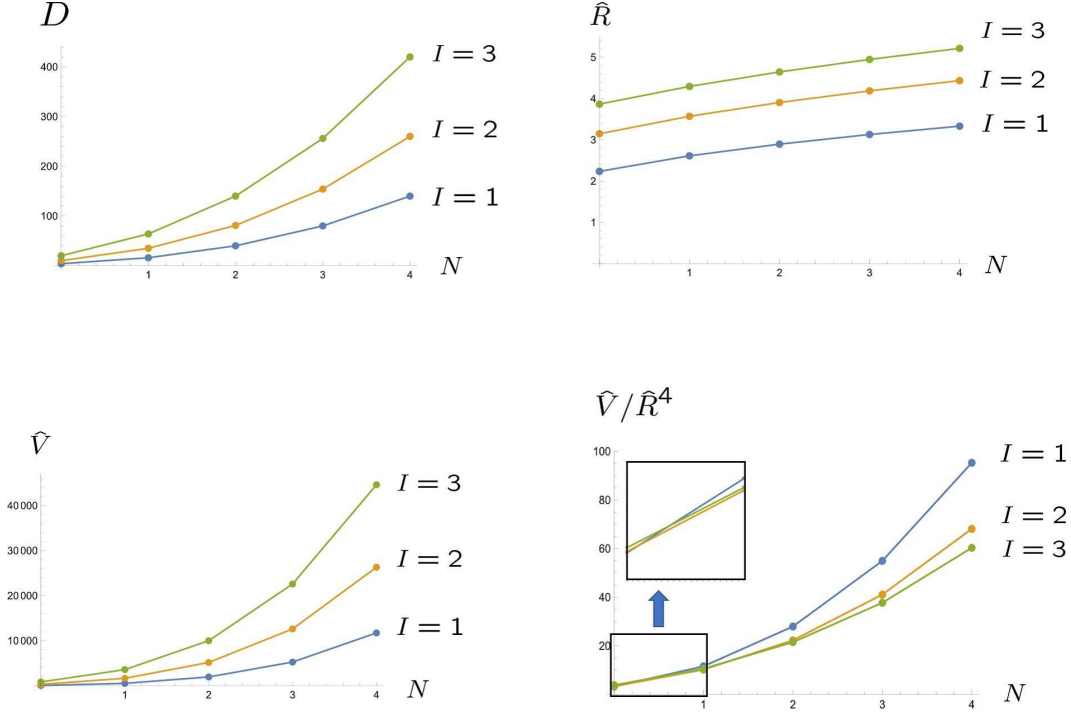


Figure 13: Behaviors of the matrix size D (the upper left), the radius (the upper right) and the potential energy (the lower left) and the potential energy density (the lower right).

Under the scaling $A_i \rightarrow \sqrt{\rho} A_i$, the parameter ρ turns to the overall scale factor of the action and does not have any physical effect. We will take $\rho = 1$:

$$S_{\text{mass}} = -\frac{1}{4} \text{tr}([A_a, A_b]^2) - \frac{1}{2} \text{tr}(A_a^2). \quad (152)$$

The equations of motion are derived as

$$[[A_a, A_b], A_b] = A_a. \quad (153)$$

Using (143), we readily see that the nested fuzzy four-spheres realize new classical solutions:²²

$$A_a^{\text{cl}} = \alpha_{\text{mass}}(N, I) \hat{X}_a^{[N]}, \quad (154)$$

where the non-commutative parameter is given by

$$\alpha_{\text{mass}}(N, I) \equiv \frac{c_3(N, I)^{1/3}}{\sqrt{2(c_1(N, I) - c_2(N, I))}}. \quad (155)$$

The non-commutative parameter α is a parameter-dependent quantity unlike the case of the fuzzy two-sphere solution (see Appendix B.2). This brings specific physical properties to the fuzzy four-sphere solu-

²²Fuzzy two-sphere and fuzzy torus are also solutions of Eq.(153) [95].

tions. The physical quantities (150) are evaluated as²³

$$\text{radius} : R_{\text{mass}} \equiv \sqrt{\frac{c_1}{2(c_1 - c_2)}} \quad (A_a^{\text{cl}} A_a^{\text{cl}} = R_{\text{mass}}^2 \mathbf{1}), \quad (157a)$$

$$\text{action} : S_{\text{mass}}^{\text{cl}} = \left(-\frac{1}{4} + \frac{1}{2}\right) \text{tr}([A_a^{\text{cl}}, A_b^{\text{cl}}]^2) = \frac{1}{4} \text{tr}([A_a^{\text{cl}}, A_b^{\text{cl}}]^2) = -\frac{1}{8} \frac{c_1}{c_1 - c_2} D = -\frac{1}{4} R_{\text{mass}}^2 D, \quad (157b)$$

$$\text{action density} : \frac{S_{\text{mass}}^{\text{cl}}}{R_{\text{mass}}^4} = -\frac{c_1 - c_2}{2c_1} D = -\frac{1}{4R_{\text{mass}}^2} D = -\frac{V}{\hat{R}^4}. \quad (157c)$$

The behaviors of Eqs.(155) and (157) are shown in Fig.14. Similar to the case of $\hat{X}_a^{[N]}$ in Sec.7.1, the action densities (the lower right of Fig.14) exhibit qualitatively distinct behaviors to the fuzzy two-sphere (Fig.17).

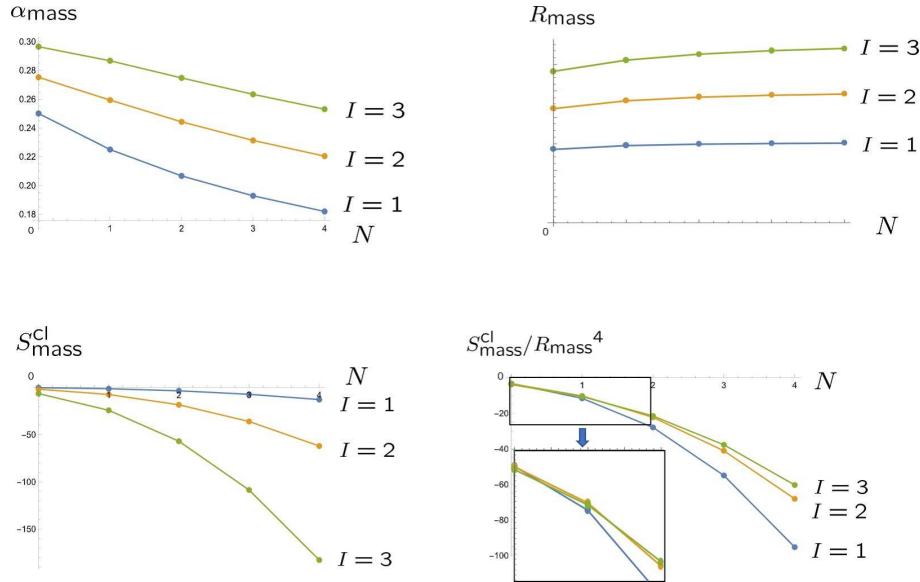


Figure 14: Behaviors of Eqs.(155) and (157).

7.2.2 With a fifth-rank Chern-Simons term

We next consider the Yang-Mills matrix model with a fifth-rank Chern-Simons term [95]

$$S_{\text{CS}}[X_a] = -\frac{1}{4} \text{tr}([X_a, X_b]^2) + \frac{\lambda}{5} \epsilon_{abcde} \text{tr}(X_a X_b X_c X_d X_e). \quad (158)$$

The coupling constant λ can be absorbed in the action when scaling A_a as $A_a \rightarrow \frac{1}{\lambda} \cdot A_a$. We then set $\lambda = 1$ and deal with the following action:

$$S_{\text{CS}} = -\frac{1}{4} \text{tr}([A_a, A_b]^2) + \frac{1}{5} \epsilon_{abcde} \text{tr}(A_a A_b A_c A_d A_e). \quad (159)$$

²³In the lowest Landau level ($N = 0$), Eq.(157) is reduced to

$$R_{\text{mass}} = \frac{1}{4} \sqrt{I(I+4)}, \quad S_{\text{mass}}^{\text{cl}} = -\frac{1}{384} I(I+1)(I+2)(I+3)(I+4), \quad \frac{S_{\text{mass}}^{\text{cl}}}{R_{\text{mass}}^4} = -\frac{2}{3} \frac{(I+1)(I+2)(I+3)}{I(I+4)}. \quad (156)$$

The equations of motion are given by

$$[[A_a, A_b], A_c] = -\epsilon_{abcde} A_b A_c A_d A_e. \quad (160)$$

From (143), we easily obtain new classical solutions as

$$A_a^{\text{cl}} = \alpha_{\text{CS}}(N, I) \hat{X}_a^{[N]} \quad (161)$$

with

$$\alpha_{\text{CS}}(N, I) \equiv \frac{1}{12} \frac{c_1(N, I) - c_2(N, I)}{c_3(N, I)^{2/3}}, \quad (162)$$

and²⁴

$$\text{radius : } R_{\text{CS}} \equiv \frac{1}{12} \frac{(c_1 - c_2)c_1^{1/2}}{c_3} = \alpha_{\text{CS}} \hat{R} \quad (A_a^{\text{cl}} A_a^{\text{cl}} = \alpha_N^2 \hat{X}_a^{[N]} \hat{X}_a^{[N]} = R_{\text{CS}}^2 \mathbf{1}_{D(N, I)}), \quad (166a)$$

$$\text{action : } S_{\text{CS}}^{\text{cl}} \equiv S_{\text{CS}}[A_a^{\text{cl}}] = -\overbrace{\left(\frac{1}{4} - \frac{1}{5}\right)}^{\frac{1}{20}} \text{tr}([A_a^{\text{cl}}, A_b^{\text{cl}}]^2) = \frac{1}{5} \alpha_{\text{CS}}^4 V = \frac{1}{10} \frac{(c_1 - c_2)^5 c_1}{(12c_3)^4} D(N, I), \quad (166b)$$

$$\text{action density : } \frac{S_{\text{CS}}^{\text{cl}}}{R_{\text{CS}}^4} = \frac{1}{10} \frac{c_1 - c_2}{c_1} D(N, I) = \frac{1}{5} \frac{V}{\hat{R}_{\text{CS}}^4} = -\frac{1}{5} \frac{S_{\text{mass}}^{\text{cl}}}{R_{\text{mass}}^4}. \quad (166c)$$

Figure 15 depicts the behaviors of Eq.(166). There are three noteworthy points. First, the order of α_{CS} for $I = 1, 2, 3$ is the reverse of that of α_{mass} (the upper left in Fig.14). Second, the order of magnitudes of R_{CS} for $I = 1, 2, 3$ is reversed between $N = 0$ and $N = 2$. Last, the order of magnitudes of both $S_{\text{CS}}^{\text{cl}}$ (lower left in Fig.15) and $S_{\text{CS}}^{\text{cl}}/R_{\text{CS}}^4$ (lower right in Fig.15) of $N = 0$ for $I = 1, 2, 3$ is the reverse of those of $N \geq 1$. Thus, the lowest Landau level matrix geometry ($N = 0$) and the newly obtained higher Landau level matrix geometries ($N \geq 1$) exhibit qualitatively distinct physical properties. It is rather curious that, while the matrix size D is a monotonically increasing function about I and the quantities such as R_{CS} and $S_{\text{CS}}^{\text{cl}}$ are expected to show similar behaviors the higher Landau level matrix geometries, *i.e.* the nested fuzzy four-spheres, do not follow this anticipation.

8 Even higher dimensions

We here investigate higher Landau level matrix geometries in even higher dimensions. The associated higher form gauge field and Yang-Mills matrix model are also discussed.

8.1 Landau level matrix geometries

It is known that (unnested) higher dimensional fuzzy spheres are realized as the lowest Landau level matrix geometries in higher dimensional Landau models [80, 79, 44]. Since $S^d \simeq SO(d+1)/SO(d)$, the

²⁴In the lowest Landau level ($N = 0$), we have

$$\alpha = \frac{2}{3} \left(\frac{3}{I+2} \right)^{2/3}, \quad A_a^{\text{cl}} = \alpha \hat{X}_a^{[0]} = \frac{2}{I+2} \Gamma_a, \quad (163)$$

which satisfies

$$[A_a^{\text{cl}}, A_b^{\text{cl}}, A_c^{\text{cl}}, A_d^{\text{cl}}] = -\left(\frac{8}{I+2} \right)^2 \epsilon_{abcde} A_e^{\text{cl}}. \quad (164)$$

Equation (166) reproduces the results of Ref.[95] for $N = 0$:

$$R_{\text{CS}} = \frac{2\sqrt{I(I+4)}}{I+2}, \quad S_{\text{CS}}^{\text{cl}} = \frac{32}{15} \frac{I(I+1)(I+3)(I+4)}{(I+2)^3}, \quad \frac{S_{\text{CS}}^{\text{cl}}}{R_{\text{CS}}^4} = \frac{2}{15} \frac{(I+1)(I+2)(I+3)}{I(I+4)}. \quad (165)$$

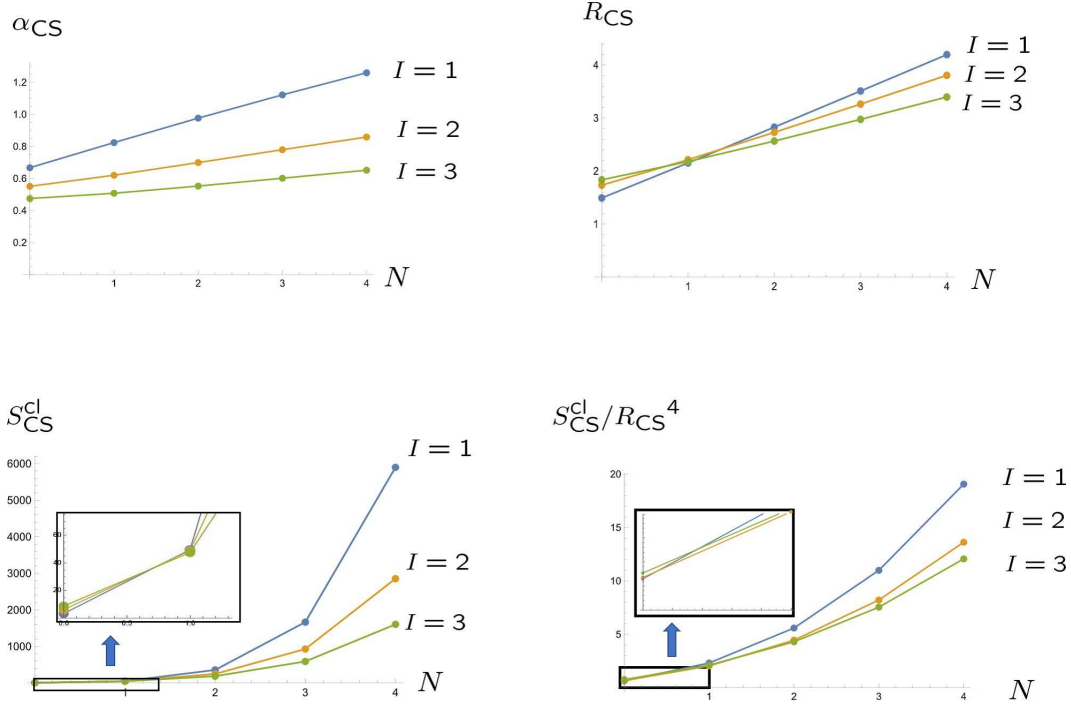


Figure 15: Behaviors of the non-commutative scale (the upper left), the radius (the upper right), the action (the lower left) and the action density (the lower right).

corresponding gauged quantum mechanics is given by the $SO(d+1)$ Landau model in the $SO(d)$ non-Abelian monopole background. The matrix coordinates in the lowest Landau level are given by the fully symmetric combination of the $SO(2k+1)$ gamma matrices:

$$X_a^{[N=0]} = \frac{1}{I+2k} (\gamma_a \otimes 1 \otimes \cdots \otimes 1 + 1 \otimes \gamma_a \otimes \cdots \otimes 1 + \cdots + 1 \otimes 1 \otimes \cdots \otimes \gamma_a)_{\text{sym}}, \quad (167)$$

which satisfy the $Spin(2k+2)$ Lie algebraic commutation relations together with the $SO(2k)$ generators.

The higher Landau level geometries in the $SO(d+1)$ Landau model have not been investigated so far. Though it is in principle possible to derive higher Landau level matrix geometries by following the present non-commutative scheme, it is rather laborious to solve the eigenvalue problem of the higher dimensional Landau Hamiltonian. Furthermore, the resulting matrix structures may be mathematically too involved to deduce useful information about the higher dimensional non-commutative geometry. Therefore, we will engage in a somewhat speculative yet more general discussion based on group theory. Let us focus on the following $SO(2k+1)$ irreducible representation

$$[l_1, l_2, \cdots, l_k]_{SO(2k+1)} = [N+I, I, \cdots, I], \quad (168)$$

which corresponds to the N th Landau level eigenstates of the $SO(2k+1)$ Landau model studied in Refs.[79, 44]. From group representation theory, the corresponding degeneracy is given by

$$D(N, I)_{SO(2k+1)} = \frac{2N+I+2k-1}{(2k-1)!!} \frac{(N+k-1)!}{N!(k-1)!} \frac{(I+2k-3)!!}{(I-1)!!} \frac{(N+I+2k-2)!}{(N+I+k-1)!} \prod_{l=1}^{k-2} \frac{(I+2l)!}{(I+l)!} \prod_{l=1}^{k-1} \frac{l!}{(2l)!}. \quad (169)$$

Meanwhile, for the one dimension lower $SO(2k)$ Landau model, the Landau levels consist of sub-bands [80]. The eigenstates of the s band of the n th Landau level constitute an $SO(2k)$ irreducible representation:

$$[l_1, l_2, \dots, l_{k-1}, l_k]_{SO(2k)} = [n + \frac{I}{2}, \frac{I}{2}, \dots, \frac{I}{2}, s], \quad (170)$$

with degeneracy

$$d(n, I, s)_{SO(2k)} = \frac{(2n + I + 2k - 2)^2 - 4s^2}{4(k-1)^2} \cdot \prod_{2 \leq i \leq k-1} \frac{(n + I + 2k - i - 1)(n + i - 1)}{(2k - i - 1)(i - 1)} \cdot \prod_{2 \leq i < j \leq k-1} \frac{I + 2k - i - j}{2k - i - j} \cdot \prod_{2 \leq i \leq k-1} \frac{(I + 2k - 2i)^2 - 4s^2}{4(k - i)^2}. \quad (171)$$

There exists an *exact* relation between the degeneracies (169) and (171):

$$D(N, I)_{SO(2k+1)} = \sum_{n=0}^N \sum_{s=-I/2}^{I/2} d(n, I, s)_{SO(2k)}. \quad (172)$$

Equation (172) signifies a higher dimensional generalization of Eq.(45) and implies that the $SO(2k+1)$ irreducible representation is constructed by adding up the $SO(2k)$ sectors from $n = 0$ to $n = N$ each of which is made of $s = I/2, \dots, -I/2$. Since the geometric structure of the fuzzy manifold reflects on the structure of the irreducible representation, the matrix geometry of the N th Landau level is expected to exhibit $N+1$ nested fuzzy structures in arbitrary dimensions, just like the nested fuzzy four-sphere. It is also reasonable to consider that fuzzy $(2k-1)$ -spheres are embedded within the nested fuzzy $2k$ -sphere.

8.2 Higher form gauge field and Yang-Mills matrix model

The lowest Landau level matrix geometry in $2k$ dimension is associated with a generalized Hopf maps [39] and are described by both the $SO(2k+2)$ Lie algebra and quantum Nambu $2k$ algebra. Meanwhile, the matrix coordinates in the higher Landau levels are not associated with the generalized Hopf map but are covariant under the $SO(2k+1)$ transformation like the lowest Landau level matrix coordinates. Therefore, the higher Landau level matrix coordinates will not conform with the Lie algebraic description but instead is described by the quantum Nambu algebra exclusively:

$$[X_{a_1}, X_{a_2}, \dots, X_{a_{2k}}] = (2k)! i^k c_3 \epsilon_{a_1 a_2 \dots a_{2k+1}} X_{2k+1}. \quad (173)$$

When one adopt more general irreducible representations beyond Eq.(168), the corresponding fuzzy manifold will exhibit a more exotic quantum geometry than the nested fuzzy structure, however, due to the existence of the $SO(2k+1)$ covariance, the matrix coordinates will also adhere to the quantum Nambu algebra (173).

Interestingly, “magnetic field” appears on the right-hand side of (173) [79], which signifies the tensor monopole field strength :

$$G_{2k} = \frac{1}{2^{k+1} \Gamma(2k+1)} \epsilon_{a_1 a_2 \dots a_{2k+1}} x_{a_{2k+1}} dx_{a_1} \wedge dx_{a_2} \wedge \dots \wedge dx_{a_{2k}}. \quad (174)$$

The existence of the higher form gauge field behind the quantum Nambu geometry is thus glimpsed. One may wonder where such a higher gauge symmetry comes from, where as the present quantum mechanical system only has the $SO(2k)$ gauge symmetry. Indeed, the tensor monopole gauge field is directly obtained from the $SO(2k)$ monopole gauge field through the Chern-Simons term [79].

The (unnested) fuzzy $2k$ -sphere realizes a solution of [22]

$$[[X_a, X_b], X_b] = i^k \epsilon_{aa_2a_3 \dots a_{2k+1}} X_{a_2} X_{a_3} \dots X_{a_{2k+1}}, \quad (175)$$

which is derived from the Yang-Mills matrix model with a $2k + 1$ rank Chern-Simons term,

$$S_{\text{CS}}[X_a] = -\frac{1}{4} \text{tr}([X_a, X_b]^2) - i^k \frac{1}{2k+1} \text{tr}(\epsilon_{aa_2a_3 \dots a_{2k+1}} X_{a_1} X_{a_2} \dots X_{a_{2k+1}}). \quad (176)$$

Since the equations of motion are concerned with the covariance of the matrix coordinates, it is anticipated that the nested fuzzy $2k$ -spheres realize classical solutions of Eq.(175). The action of for the fuzzy $2k$ -sphere solution is given by

$$S_{\text{CS}}(X_a = X_a^{\text{cl}}) = \left(-\frac{1}{4} + \frac{1}{2k+1}\right) \text{tr}([X_a^{\text{cl}}, X_b^{\text{cl}}]^2) = \frac{2k-3}{2k+1} V(X_a^{\text{cl}}), \quad (177)$$

where

$$V(X_a^{\text{cl}}) \equiv -\frac{1}{4} \text{tr}([X_a^{\text{cl}}, X_b^{\text{cl}}]^2). \quad (178)$$

While the signs of $S_{\text{CS}}(X_a^{\text{cl}})$ and $V(X_a^{\text{cl}})$ are opposite for $k = 1$, they have the same sign for $k \geq 2$, as we have seen, for $k = 2$, in Eq. (166b).

9 Summary and discussions

Based on the insight obtained from the emergent fuzzy geometry in the simple $SO(3)$ Landau model, we proposed a novel non-commutative scheme for generating the matrix geometries for arbitrary manifolds of the coset type G/H . In the present approach, manifolds need not be either symplectic or even dimensional unlike the conventional non-commutative schemes. We explicitly derived the matrix geometries for S^4 by utilizing the $SO(5)$ Landau model. The emergent matrix geometries in higher Landau levels realize pure quantum Nambu geometries in which matrix coordinates are not closed within the canonical formalism of the Lie algebra but are described only by introducing the quantum Nambu algebra. We also demonstrated that such pure quantum matrix geometries manifest new solutions of the Yang-Mills matrix models. The particular features of the nested quantum geometry, such as the internal matrix geometries, continuum limit, and classical counterpart, were clarified. The pure Nambu matrix geometries are common to the higher Landau levels of the Landau models in arbitrary dimensions.

The conventional scheme is based on the spirit of quantization of classical (symplectic) manifolds, *i.e.*, the replacement of the Poisson bracket with the commutator, where as the present non-commutative scheme is largely based on the mathematical structure of the Hilbert space behind quantum mechanics from the beginning. In this sense, the present scheme is considered to be a quantum-oriented non-commutative scheme. That is the reason why we obtained the pure quantum geometry. We showed this non-commutative scheme is practically useful in deriving novel solutions of the Matrix models. As Matrix model solutions, the nested matrix geometries exhibit quantitatively distinct behaviors with the unnested fuzzy four-sphere.

The discovery of the novel quantum Nambu matrix geometries now brings various open questions, such as brane construction, relation to tachyon condensation [96, 97], realization in the Nahm equation in higher energy physics. The higher form gauge field implied by the quantum Nambu algebra is closely related to the higher Berry phase [98, 99] whose usefulness is getting appreciated in the very recent studies of strongly correlated many-body systems. It would be intriguing to speculate on the role of quantum Nambu geometry in condensed matter physics. We also add that the present scheme itself should be appropriately generalized to treat less symmetric fuzzy objects, while we studied highly symmetric objects in this work.

To the best of the author's knowledge, this work is the first example of quantum matrix geometry found in the analysis of the Landau models being practically applied to the solutions of the M(atr)ix models.

M(atrix) theory is assumed to describe the physics at the Planck scale of 10^{19} GeV, while the Landau models or the quantum Hall effect are about the low temperature physics at milli-electron volt. It is rather amazing that same mathematics work in both physics with such a huge energy gap.

Acknowledgments

This work was supported by JSPS KAKENHI Grant No. 21K03542.

A Groenewold-Moyal plane from planar Landau model

We demonstrate a realization of the Groenewold-Moyal plane in higher Landau levels. Let us consider a 2D plane subject to a constant perpendicular magnetic field:

$$\partial_x A_y - \partial_y A_x = B. \quad (179)$$

We employ the gauge-independent relation (179), and so all of the following results are also gauge independent. The covariant derivatives and the center-of-mass coordinates are respectively constructed as

$$D_i = \frac{\partial}{\partial x_i} + iA_i, \quad X_i^{\text{CM}} = x_i + i\frac{1}{B}\epsilon_{ij}D_j \quad (i = 1, 2), \quad (180)$$

which satisfy two independent commutation relations:

$$[D_x, D_y] = iB, \quad [X^{\text{CM}}, Y^{\text{CM}}] = i\frac{1}{B}, \quad [D_i, X_j^{\text{CM}}] = 0. \quad (181)$$

We then realize two sets of creation and annihilation operators as

$$a = i\frac{1}{\sqrt{2B}}(D_x - iD_y), \quad a^\dagger = i\frac{1}{\sqrt{2B}}(D_x + iD_y), \quad b = \sqrt{\frac{B}{2}}(X^{\text{CM}} + iY^{\text{CM}}), \quad b^\dagger = \sqrt{\frac{B}{2}}(X^{\text{CM}} - iY^{\text{CM}}), \quad (182)$$

which satisfy

$$[a, a^\dagger] = [b, b^\dagger] = 1, \quad [a, b] = [a, b^\dagger] = 0. \quad (183)$$

The Hamiltonian of the planar Landau model is given by

$$H = -\frac{1}{2M}(D_x^2 + D_y^2) = \frac{B}{M}(a^\dagger a + \frac{1}{2}). \quad (184)$$

The corresponding energy Landau levels and the eigenstates are

$$E_N = \frac{B}{M}(N + \frac{1}{2}), \quad |N, m\rangle = \frac{1}{\sqrt{N!} m!} a^{\dagger N} b^{\dagger m} |0\rangle \quad (N, m = 0, 1, 2, \dots). \quad (185)$$

Using

$$x = X^{\text{CM}} - i\frac{1}{B}D_y = \frac{1}{\sqrt{2B}}(b + b^\dagger) - i\frac{1}{\sqrt{2B}}(a - a^\dagger), \quad y = Y^{\text{CM}} + i\frac{1}{B}D_x = -i\frac{1}{\sqrt{2B}}(b - b^\dagger) + \frac{1}{\sqrt{2B}}(a + a^\dagger), \quad (186)$$

we readily evaluate the matrix elements of x and y :

$$\begin{aligned} \langle N, m|x|N', m'\rangle &= \frac{1}{\sqrt{2B}}(\sqrt{m'} \delta_{m, m'-1} + \sqrt{m'+1} \delta_{m, m'+1}) \delta_{N, N'} - i\frac{1}{\sqrt{2B}}(\sqrt{N'} \delta_{N, N'-1} - \sqrt{N'+1} \delta_{N, N'+1}) \delta_{m, m'}, \\ \langle N, m|y|N', m'\rangle &= -i\frac{1}{\sqrt{2B}}(\sqrt{m'} \delta_{m, m'-1} - \sqrt{m'+1} \delta_{m, m'+1}) \delta_{N, N'} + \frac{1}{\sqrt{2B}}(\sqrt{N'} \delta_{N, N'-1} + \sqrt{N'+1} \delta_{N, N'+1}) \delta_{m, m'}. \end{aligned} \quad (187)$$

The intra-Landau level matrix coordinates are then obtained as

$$\begin{aligned}(X^{(N)})_{mm'} &\equiv \langle N, m | x | N, m' \rangle = \frac{1}{\sqrt{2B}} (\sqrt{m'} \delta_{m, m'-1} + \sqrt{m'+1} \delta_{m, m'+1}), \\ (Y^{(N)})_{mm'} &\equiv \langle N, m | y | N, m' \rangle = -i \frac{1}{\sqrt{2B}} (\sqrt{m'} \delta_{m, m'-1} - \sqrt{m'+1} \delta_{m, m'+1}),\end{aligned}\quad (188)$$

or

$$X^{(N)} = \frac{1}{\sqrt{2B}} \begin{pmatrix} 0 & \sqrt{1} & 0 & 0 & 0 & 0 \\ \sqrt{1} & 0 & \sqrt{2} & 0 & 0 & 0 \\ 0 & \sqrt{2} & 0 & \sqrt{3} & 0 & 0 \\ 0 & 0 & \sqrt{3} & 0 & \ddots & 0 \\ 0 & 0 & 0 & \ddots & 0 & \ddots \end{pmatrix}, \quad Y^{(N)} = i \frac{1}{\sqrt{2B}} \begin{pmatrix} 0 & -\sqrt{1} & 0 & 0 & 0 & 0 \\ \sqrt{1} & 0 & -\sqrt{2} & 0 & 0 & 0 \\ 0 & \sqrt{2} & 0 & -\sqrt{3} & 0 & 0 \\ 0 & 0 & \sqrt{3} & 0 & \ddots & 0 \\ 0 & 0 & 0 & \ddots & 0 & \ddots \end{pmatrix}. \quad (189)$$

Notice that (189) does not depend on the Landau level index N , and the matrix coordinates satisfy

$$[X^{(N)}, Y^{(N)}] = i \frac{1}{B} \mathbf{1}. \quad (190)$$

Obviously, the dimensionless coordinates, $\hat{X}^{(N)} = \sqrt{B} X^{(N)}$ and $\hat{Y}^{(N)} = \sqrt{B} Y^{(N)}$, satisfy the Heisenberg-Weyl algebra together with $\mathbf{1}$:

$$[\hat{X}^{(N)}, \hat{Y}^{(N)}] = i \mathbf{1}, \quad [\hat{X}^{(N)}, \mathbf{1}] = [\hat{Y}^{(N)}, \mathbf{1}] = 0. \quad (191)$$

We have thus confirmed the emergence of the Groenewold-Moyal plane in *any* Landau level.

B Two-sphere matrix coordinates in Yang-Mills matrix models

For comparison with the fuzzy four-sphere (Sec.7), we revisit matrix model the analyses of fuzzy two-sphere [101, 100], clarifying physical properties of the matrix coordinates in the $SO(3)$ Landau model.

B.1 Basic properties

The N th Landau level matrix coordinates $X_i^{(N)}$ (8) satisfy the following relations²⁵

$$X_i^{(N)} X_i^{(N)} = c_1(N, I) \mathbf{1}_{D(N, I)}, \quad (192a)$$

$$X_j^{(N)} X_i^{(N)} X_j^{(N)} = c_2(N, I) X_i^{(N)}, \quad (192b)$$

$$\epsilon_{ijk} X_j^{(N)} X_k^{(N)} = 2i c_3(N, I) X_i^{(N)}, \quad (192c)$$

where

$$D(N, I) = I + 2N + 1, \quad (193)$$

and

$$c_1(N, I) \equiv \frac{I^2}{(I + 2N)(I + 2N + 2)}, \quad (194a)$$

$$c_2(N, I) \equiv \frac{I^2}{(I + 2N)^2 (I + 2N + 2)^2} ((I + 2N)(I + 2N + 2) - 4), \quad (194b)$$

$$c_3(N, I) \equiv \frac{I}{(I + 2N)(I + 2N + 2)}. \quad (194c)$$

²⁵In the literatures on matrix models, it is common to denote the variables D and I as N and n , respectively.

These c s are not independent quantities; instead, they satisfy

$$c_1 - c_2 = 4c_3^2. \quad (195)$$

From (194), we readily have

$$-\frac{1}{4}[X_i^{(N)}, X_j^{(N)}]^2 = \frac{1}{2}(c_2 - c_2)c_1 \mathbf{1}_D \quad (196)$$

and

$$V(N, I) = -\frac{1}{4}\text{tr}([X_i^{(N)}, X_j^{(N)}]^2) = \frac{1}{2}(c_2 - c_2)c_1 D = 2 \frac{I^4}{(I + 2N)^3(I + 2N + 2)^3} (2N + I + 1). \quad (197)$$

The behaviors of (194) and (197) are shown in Fig.16.

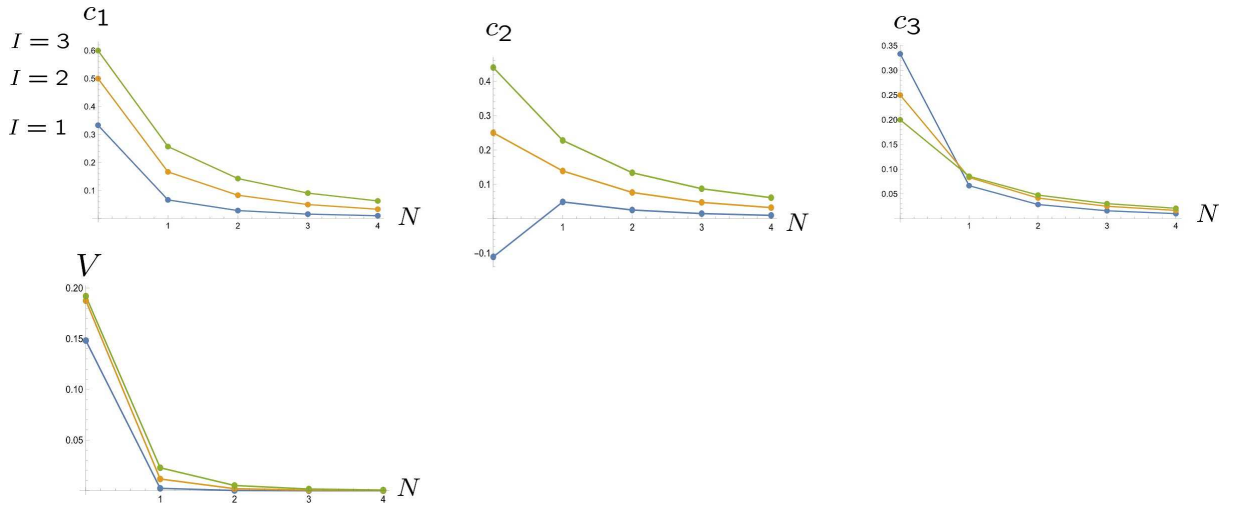


Figure 16: The blue, orange and green lines correspond to $I = 1, 2, 3$ of Eqs.(194) and (197).

We introduce “normalized” matrix coordinates that satisfy the $SU(2)$ algebra

$$[\hat{X}_i^{(N)}, \hat{X}_j^{(N)}] = 2i\epsilon_{ijk}\hat{X}_k^{(N)} \quad (198)$$

as

$$\hat{X}_i^{(N)} = \frac{1}{c_3(N, I)} X_i^{(N)} = 2S_i^{(\frac{I}{2}+N)}. \quad (199)$$

Notice that $\hat{X}_i^{(N)}$ depend on the $SU(2)$ index $l = N + \frac{I}{2}$ rather than N and I , separately. Several important physical quantities are evaluated as

$$\text{radius} : \hat{R} = \frac{\sqrt{c_1}}{c_3} = \sqrt{(I + 2N)(I + 2N + 2)}, \quad (200a)$$

$$\text{potential energy} : V = -\frac{1}{4}\text{tr}([\hat{X}_i^{(N)}, \hat{X}_j^{(N)}]^2) = \frac{2}{c_3^2} c_1 D(N, I) = 2(I + 2N)(I + 2N + 1)(I + 2N + 2), \quad (200b)$$

$$\text{potential energy density} : \frac{V}{\hat{R}^2} = 2D(N, I) = 2(I + 2N + 1). \quad (200c)$$

The potential energy density is simply the twice the matrix size of the fuzzy two-sphere.

B.2 Matrix model analysis

Yang-Mills matrix models with a mass term and with a third-rank Chern-Simons term are given by

$$S_{\text{mass}} = -\frac{1}{4}\text{tr}([A_i, A_j]^2) - \frac{1}{2}\text{tr}(A_i^2), \quad S_{\text{CS}} = -\frac{1}{4}\text{tr}([A_i, A_j]^2) + i\frac{1}{3}\epsilon_{ijk}\text{tr}(A_i A_j A_k), \quad (201)$$

and the corresponding equations of motion are respectively

$$[[A_i, A_j], A_j] = A_i, \quad [[A_i, A_j], A_j] = -i\epsilon_{ijk}A_j A_k, \quad (202)$$

The fuzzy two-sphere is realized as a solution:

$$A_i^{\text{cl}} = \alpha_{\text{mass}} \hat{X}_i^{(N)}, \quad A_i^{\text{cl}} = \alpha_{\text{CS}} \hat{X}_i^{(N)}, \quad (203)$$

with

$$\alpha_{\text{mass}} \equiv \frac{1}{2\sqrt{2}}, \quad \alpha_{\text{CS}} \equiv \frac{1}{4}. \quad (204)$$

Notice that both coefficients, α_{mass} and α_{CS} , are constant unlike the case of the fuzzy four-sphere solutions (see Sec.7). The classical solutions (203) have the following properties:

$$\text{radius} : R_{\text{mass}} \equiv \alpha_{\text{mass}} \hat{R} \quad (A_i^{\text{cl}} A_i^{\text{cl}} = R_{\text{mass}}^2 \mathbf{1}), \quad R_{\text{CS}} \equiv \alpha_{\text{CS}} \hat{R} \quad (A_i^{\text{cl}} A_i^{\text{cl}} = R_{\text{CS}}^2 \mathbf{1}), \quad (205a)$$

$$\text{action} : S_{\text{mass}}^{\text{cl}} = \overbrace{\left(-\frac{1}{4} + \frac{1}{2}\right)}^{=1/4} \text{tr}([A_i^{\text{cl}}, A_i^{\text{cl}}]^2) = -\alpha_{\text{mass}}^4 V, \quad S_{\text{CS}}^{\text{cl}} \equiv S_{\text{CS}}[A_i^{\text{cl}}] = \overbrace{\left(-\frac{1}{4} + \frac{1}{3}\right)}^{=1/12} \text{tr}([A_i^{\text{cl}}, A_j^{\text{cl}}]^2) = -\frac{1}{3}\alpha_{\text{CS}}^4 V, \quad (205b)$$

$$\text{action density} : \frac{S_{\text{mass}}^{\text{cl}}}{R_{\text{mass}}^2} = -\alpha_{\text{mass}}^2 \frac{V}{\hat{R}^2} = -\frac{1}{4}D, \quad \frac{S_{\text{CS}}^{\text{cl}}}{R_{\text{CS}}^2} = -\frac{1}{3}\alpha_{\text{CS}}^2 \frac{V}{\hat{R}^2} = -\frac{1}{24}D. \quad (205c)$$

See Fig.17 for the behaviors of these quantities.

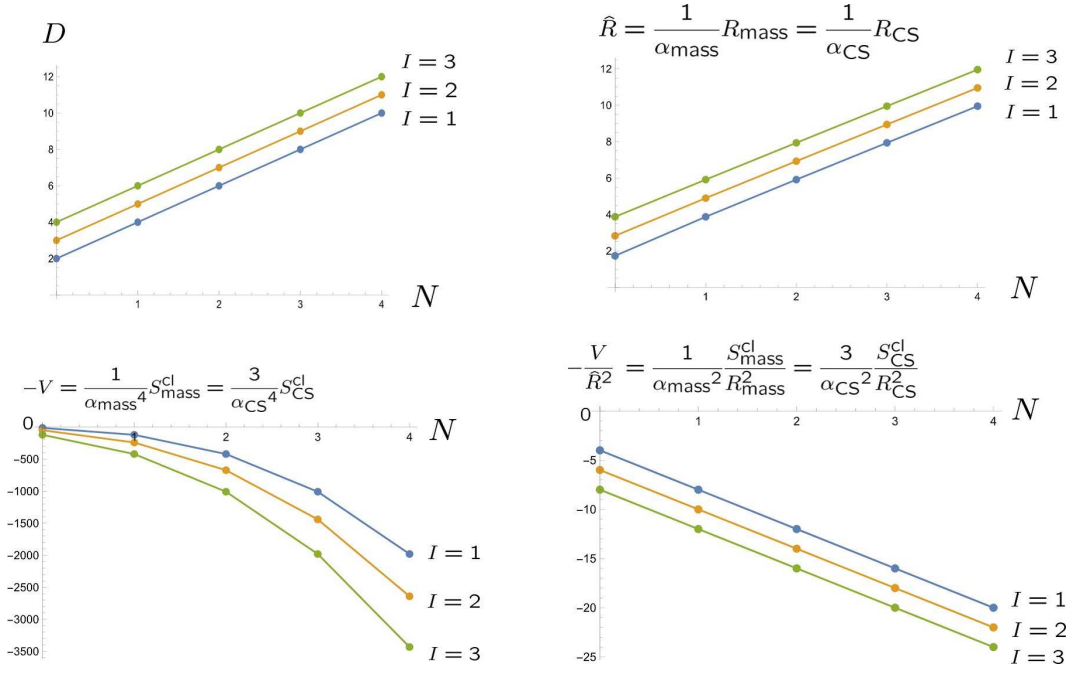


Figure 17: Physical quantities of the fuzzy two-spheres. All quantities monotonically increase or decrease as N and I increase.

C Matrix coordinates and $SO(5)$ generators for $(N, I) = (1, 1)$

The following 16×16 matrices denote the matrix coordinates for $(N, I) = (1, 1)$:

[illegible]

The $SO(5)$ generators $(N, I) = (1, 1)$ are

[illegible]

[illegible]

[1] Hartland S. Snyder, “*Quantized space-time*”, Phys.Rev. 67 (1947) 38.

- [2] C. N. Yang, “*On quantized space-time*”, Phys.Rev. 72 (1947) 874.
- [3] Miao Li, Yong-Shi Wu, “*Physics in Noncommutative World: Field Theories*”, Rinton Press (2002).
- [4] Alain Connes, “*Noncommutative Geometry*”, Academic Press (1994).
- [5] S. Twareque Ali, Miroslav Englis, “*Quantization Methods: A Guide for Physicists and Analysts*”, Rev. Math. Phys. 17 (2005) pp.391 - 490; math-ph/0405065.
- [6] Thomas L. Curtright, Cosmas K. Zachos, “*Quantum Mechanics in Phase space*”, Asia Pacific Physics Newsletter, 1 (2012) pp 37-46; arXiv:1104.5269.
- [7] Cosmas K. Zachos, David B. Fairlie, Thomas L. Curtright, “*Quantum Mechanics in Phase Space*”, World Scientific Pub Co Inc (2006).
- [8] Anirban Basu, Jeffrey A. Harvey, “*The M2-M5 Brane System and a Generalized Nahm’s Equation*”, Nucl.Phys. B713 (2005) 136-150; hep-th/0412310.
- [9] Jonathan Bagger, Neil Lambert, “*Modeling Multiple M2’s*”, Phys.Rev.D75 (2007) 045020; hep-th/0611108.
- [10] Andreas Gustavsson, “*Algebraic structures on parallel M2-branes*”, Nucl.Phys.B811 (2009) 66-76; arXiv:0709.1260.
- [11] Jonathan Bagger, Neil Lambert, “*Gauge Symmetry and Supersymmetry of Multiple M2-Branes*”, Phys.Rev.D77 (2008) 065008; arXiv:0711.0955.
- [12] T. Banks, W. Fischler, S. Shenker and L. Susskind, “*M theory as a matrix model: a conjecture,*”, Phys.Rev.D55 (1997) 5112; hep-th/9610043.
- [13] N. Ishibashi, H. Kawai, Y. Kitazawa and A. Tsuchiya, “*A Large N reduced model as super-string*”, Nucl.Phys.B498 (1997) 467; hep-th/9612115..
- [14] J. Madore, “*The Fuzzy Sphere*”, Class. Quant. Grav. 9 (1992) 69.
- [15] H. Grosse, C. Klimcik, P. Presnajder, “*On Finite 4D Quantum Field Theory in Non-Commutative Geometry*”, Commun.Math.Phys. 180 (1996) 429-438; hep-th/9602115.
- [16] Judith Castelino, Sangmin Lee, Washington Taylor, “*Longitudinal 5-branes as 4-spheres in Matrix theory*”, Nucl.Phys.B526 (1998) 334-350; hep-th/9712105.
- [17] H. Grosse and G. Reiter, “*The Fuzzy Supersphere*”, Jour. Geom. Phys. 28 (1998) 349, math-ph/9804013.
- [18] Z. Guralnik, S. Ramgoolam, “*On the Polarization of Unstable D0-Branes into Non-Commutative Odd Spheres*”, JHEP 0102 (2001) 032; hep-th/0101001.
- [19] G.Alexanian, A.P.Balachandran, G.Immirzi, B.Ydri, “*Fuzzy CP²*”, J.Geom.Phys.42 (2002) 28-53; hep-th/0103023.
- [20] P. M. Ho and S. Ramgoolam, “*Higher dimensional geometries from matrix brane constructions*”, Nucl.Phys.B 627 (2002) 266; hep-th/0111278.
- [21] Sanjaye Ramgoolam, “*Higher dimensional geometries related to fuzzy odd-dimensional spheres*”, JHEP 0210 (2002) 064; hep-th/0207111.

- [22] Yusuke Kimura, “*On higher dimensional fuzzy spherical branes*”, Nucl.Phys.B 664 (2003) 512; hep-th/0301055.
- [23] M. M. Sheikh-Jabbari, “*Tiny Graviton Matrix Theory: DLCQ of IIB Plane-Wave String Theory, A Conjecture*”, JHEP 0409 (2004) 017; hep-th/0406214.
- [24] Joakim Arnlind, Martin Bordemann, Laurent Hofer, Jens Hoppe and Hidehiko Shimada, “*Fuzzy Riemann surfaces*”, JHEP 06 (2009) 047; hep-th/0602290.
- [25] Kazuki Hasebe, “*Graded Hopf maps and fuzzy super-spheres*”, Nucl.Phys. B 853 (2011) 777; arXiv:1106.5077.
- [26] Kazuki Hasebe, “*Non-Compact Hopf Maps and Fuzzy Ultra-Hyperboloids*”, Nucl.Phys. B 865 (2012) 148-199; arXiv:1207.1968.
- [27] Washington Taylor, “*The M(atrix) model of M-theory*”, hep-th/0002016.
- [28] Washington Taylor, “*M(atrix) Theory: Matrix Quantum Mechanics as a Fundamental Theory*”, Rev.Mod.Phys.73 (2001) 419-462; hep-th/0101126.
- [29] Yoichiro Nambu, “*Generalized Hamiltonian Dynamics*”, Phys.Rev.D7 (1973) 2405-2412.
- [30] Pei-Ming Ho, Yutaka Matsuo, “*Nambu bracket and M-theory*”, Prog. Theo. Exp. Phys. (2016) 06A104; arXiv:1603.09534.
- [31] Thomas Curtright, Cosmas Zachos, “*Classical and Quantum Nambu Mechanics*”, Phys.Rev.D68 (2003) 085001; hep-th/0212267.
- [32] Joshua DeBellis, Christian Saemann, Richard J. Szabo, “*Quantized Nambu-Poisson Manifolds and n-Lie Algebras*”, J.Math.Phys.51 (2010) 122303; arXiv:1001.3275.
- [33] Y. Kawamura, “*Cubic Matrices, Generalized Spin Algebra and Uncertainty Relation*”, Prog.Theor.Phys. 110 (2003) 579-587; hep-th/0304149.
- [34] Y. Kawamura, “*Dynamical Theory of Generalized Matrices*”, Prog.Theor.Phys. 114 (2005) 669-693; hep-th/0504017.
- [35] Pei-Ming Ho, Ru-Chuen Hou, Yutaka Matsuo, “*Lie 3-Algebra and Multiple M2-branes*”, JHEP 06 (2008) 020; hep-th/0804.2110.
- [36] Leon Takhtajan, “*On Foundation of the Generalized Nambu Mechanics*”, Commun.Math.Phys. 160 (1994) 295-316; hep-th/9301111.
- [37] Giuseppe Dito, Moshe Flato, Daniel Sternheimer, Leon Takhtajan, “*Deformation Quantization and Nambu Mechanics*”, Commun.Math.Phys. 183 (1997) 1-22; hep-th/9602016.
- [38] Giuseppe Dito, Moshe Flato, “*Generalized Abelian Deformations: Application to Nambu Mechanics*”, Lett.Math.Phys. 39 (1997) 107-125; hep-th/9609114.
- [39] Kazuki Hasebe, “*Hopf Maps, Lowest Landau Level, and Fuzzy Spheres*”, SIGMA 6 (2010) 071; arXiv:1009.1192.
- [40] Dimitra Karabali, V.P. Nair, S. Randjbar-Daemi “*Fuzzy spaces, the M(atrix) model and the quantum Hall effect*”, hep-th/0407007.

- [41] S. C. Zhang and J. P. Hu, “*A Four Dimensional Generalization of the Quantum Hall Effect*”, Science 294 (2001) 823; cond-mat/0110572.
- [42] Dimitra Karabali, V.P. Nair, “*Quantum Hall Effect in Higher Dimensions*”, Nucl.Phys. B641 (2002) 533-546; hep-th/0203264.
- [43] B. A. Bernevig, J. P. Hu, N. Toumbas, S. C. Zhang, “*The eight dimensional quantum Hall effect and the octonions*”, Phys.Rev.Lett. 91 (2003) 236803; cond-mat/0306045.
- [44] K. Hasebe and Y. Kimura, “*Dimensional Hierarchy in Quantum Hall Effects on Fuzzy Spheres*”, Phys.Lett. B 602 (2004) 255; hep-th/0310274.
- [45] K. Hasebe, “*Supersymmetric Quantum Hall Effect on Fuzzy Supersphere*”, Phys.Rev.Lett. 94 (2005) 206802; hep-th/0411137.
- [46] V.P. Nair, S. Randjbar-Daemi, “*Quantum Hall effect on S^3 , edge states and fuzzy S^3/\mathbf{Z}_2* ”, Nucl.Phys. B679 (2004) 447-463; hep-th/0309212.
- [47] A. Jellal, “*Quantum Hall Effect on Higher Dimensional Spaces*”, Nucl.Phys. B725 (2005) 554-576; hep-th/0505095.
- [48] Kazuki Hasebe, “*Split-Quaternionic Hopf Map, Quantum Hall Effect, and Twistor Theory*”, Phys.Rev.D81 (2010) 041702; arXiv:0902.2523.
- [49] F. Balli, A. Behtash, S. Kurkcuoglu, G. Unal, “*Quantum Hall Effect on the Grassmannians $Gr_2(\mathbb{C}N)$* ”, Phys. Rev. D 89 (2014) 105031; arXiv:1403.3823.
- [50] Kazuki Hasebe, “*Chiral topological insulator on Nambu 3-algebraic geometry*”, Nucl.Phys. B 886 (2014) 681-690; arXiv:1403.7816.
- [51] U.H. Coskun, S. Kurkcuoglu, G.C.Toga, “*Quantum Hall Effect on Odd Spheres*”, Phys. Rev. D 95 (2017) 065021; arXiv:1612.03855.
- [52] Jonathan J. Heckman, Luigi Tizzano, “*6D fractional quantum Hall effect*”, JHEP 05 (2018) 120-179; arXiv:1708.02250.
- [53] Kazuki Hasebe, “*Relativistic Landau Models and Generation of Fuzzy Spheres*”, Int.J.Mod.Phys.A 31 (2016) 1650117; arXiv:1511.04681.
- [54] Kazuki Hasebe, “ *$SO(4)$ Landau Models and Matrix Geometry*”, Nucl.Phys. B 934 (2018) 149-211; arXiv:1712.07767.
- [55] Kazuki Hasebe, “ *$SO(5)$ Landau models and nested Nambu matrix geometry*”, Nucl.Phys. B 956 (2020) 115012; arXiv:2002.05010.
- [56] Kazuki Hasebe, “ *$SO(5)$ Landau model and 4D quantum Hall effect in the $SO(4)$ monopole background*”, Phys.Rev. D 105 (2022) 065010; arXiv:2112.03038 .
- [57] Kazuki Hasebe, “*Quantum matrix geometry in the lowest Landau level and higher Landau levels*”, PoS (CORFU2021) 239; arXiv:2212.05277 .
- [58] Goro Ishiki, Takaki Matsumoto, Hisayoshi Muraki,, “*Kähler structure in the commutative limit of matrix geometry*”, JHEP 08 (2016) 042; arXiv:1603.09146.

- [59] Tsuguhiko Asakawa, Goro Ishiki, Takaki Matsumoto, So Matsuura, Hisayoshi Muraki, “*Commutative Geometry for Non-commutative D-branes by Tachyon Condensation*”, Prog. Theor. Exp. Phys. 2018, 063B04; arXiv:1804.00161.
- [60] G. Ishiki, T. Matsumoto, H. Muraki, “*Information metric, Berry connection, and Berezin-Toeplitz quantization for matrix geometry*”, Phys. Rev. D 98 (2018) 026002; arXiv:1804.00900.
- [61] Kaho Matsuura, Asato Tsuchiya, “*Matrix geometry for ellipsoids*”, Prog. Theor. Exp. Phys. 2020, 033B05.
- [62] V. P. Nair, “*Landau-Hall states and Berezin-Toeplitz quantization of matrix algebras*”, Phys.Rev. D 102 (2020) 025015; arXiv:2001.05040.
- [63] Hiroyuki Adachi, Goro Ishiki, Takaki Matsumoto, Kaishu Saito, “*The matrix regularization for Riemann surfaces with magnetic fluxes*”, Phys. Rev. D 101 (2020) 106009; arXiv:2002.02993.
- [64] Hiroyuki Adachi, Goro Ishiki, Satoshi Kanno, “*Vector bundles on fuzzy Kähler manifolds*”, arXiv:2210.01397.
- [65] H.M. Price, O. Zilberberg, T. Ozawa, I. Carusotto, N. Goldman, “*Four-Dimensional Quantum Hall Effect with Ultracold Atoms*”, Phys. Rev. Lett. 115 (2015) 195303.
- [66] H.M. Price, O. Zilberberg, T. Ozawa, I. Carusotto, N. Goldman, “*Measurement of Chern numbers through center-of-mass responses*”, Phys. Rev. B 93 (2016) 245113.
- [67] T. Ozawa, H.M. Price, N. Goldman, O. Zilberberg, I. Carusotto, “*Synthetic dimensions in integrated photonics: From optical isolation to four-dimensional quantum Hall physics*”, Phys. Rev. A 93 (2016) 043827.
- [68] Shaojie Ma, Hongwei Jia, Yangang Bi, Shangqiang Ning, Fuxin Guan, Hongchao Liu, Chenjie Wang, Shuang Zhang, “*Gauge Field Induced Chiral Zero Mode in Five-Dimensional Yang Monopole Metamaterials*”, Phys.Rev.Lett. 130 (2023) 243801; arXiv:2305.13566.
- [69] Xingen Zheng, Tian Chen, Weixuan Zhang, Houjun Sun, Xiangdong Zhang, “*Exploring topological phase transition and Weyl physics in five dimensions with electric circuits*”, Phys.Rev.Res. 4 (2022) 033203; arXiv:2209.08492.
- [70] Sh. Ma, Y. Bi, Q. Guo, B. Yang, O. You, J. Feng, H.-B. Sun, Sh. Zhang, “*Linked Weyl surfaces and Weyl arcs in photonic metamaterials*”, Science 373 (2021) 572-576.
- [71] S. Sugawa, F. Salces-Carcoba, A. R. Perry, Y. Yue, I. B. Spielman, “*Second Chern number of a quantum-simulated non-Abelian Yang monopole*”, Science 360 (2018) 1429-1434.
- [72] T.T. Wu, C.N. Yang, “*Dirac Monopoles without Strings: Monopole Harmonics*”, Nucl.Phys. B107 (1976) 1030-1033.
- [73] F.D.M. Haldane, “*Fractional quantization of the Hall effect: a hierarchy of incompressible quantum fluid states*”, Phys. Rev. Lett. 51 (1983) 605-608.
- [74] Mikio Nakahara, “*Geometry, topology and physics*”, 2nd ed., Graduate Student Series in Physics, Institute of Physics, Bristol (2003).
- [75] Shou-Cheng Zhang, “*To see a world in a grain of sand*”, A chapter for John Wheeler’s 90’s birthday festschrift; hep-th/0210162.

- [76] Martin Schlichenmaier, “*Berezin-Toeplitz quantization and Berezin transform*”, pp. 271-287 in “*Long time behaviour of classical and quantum systems*” (Proceedings of the Bologna APTEX International Conference) Sandro Graffi and André Martinez Eds., World Scientific Publishing; math/0009219.
- [77] Chen Ning Yang, “*Generalization of Dirac’s monopole to SU_2 gauge fields*”, J. Math. Phys. 19 (1978) 320.
- [78] Chen Ning Yang, “ *$SU(2)$ monopole harmonics*”, J. Math. Phys. 19 (1978) 2622.
- [79] Kazuki Hasebe, “*Higher Dimensional Quantum Hall Effect as A-Class Topological Insulator*”, Nucl.Phys. B 886 (2014) 952-1002; arXiv:1403.5066.
- [80] Kazuki Hasebe, “*Higher (Odd) Dimensional Quantum Hall Effect and Extended Dimensional Hierarchy*”, Nucl.Phys. B 920 (2017) 475-520; arXiv:1612.05853.
- [81] Yasuhiro Abe, “*Construction of fuzzy S^4* ”, Phys.Rev. D70 (2004) 126004; hep-th/0406135.
- [82] Robert C. Myers, “*Dielectric-branes*”, JHEP 12 (1999) 022; hep-th/9910053.
- [83] Marcus Sperling, and Harold C. Steinacker, “*Covariant 4-dimensional fuzzy spheres, matrix models and higher spin*”, J.Phys. A: Math. Theor. 50 (2017) 375202; arXiv:1704.02863.
- [84] Harold Steinacker, “*One-loop stabilization of the fuzzy four-sphere via softly broken SUSY*”, JHEP 12 (2015) 115; arXiv:1510.05779.
- [85] Harald Grosse, Harold Steinacker, “*Finite Gauge Theory on Fuzzy CP^2* ”, Nucl.Phys. B707 (2005) 145-198; hep-th/0407089.
- [86] Yuri A. Kordyukov, “*Berezin-Toeplitz quantization associated with higher Landau levels of the Bochner Laplacian*”, arXiv:2012.14198.
- [87] Laurent Charles, “*Landau levels on a compact manifold*”, arXiv:2012.14190.
- [88] Goro Ishiki, “*Matrix Geometry and Coherent States*”, Phys. Rev. D 92 (2015) 046009; arXiv:1503.01230.
- [89] Lukas Schneiderbauer, Harold C Steinacker, “*Measuring finite quantum geometries via quasi-coherent states*”, Jour. Phys. A: Math. Theor. 49 (2016) 285301; arXiv:1601.08007.
- [90] Harold C. Steinacker, “*Quantum (matrix) geometry and quasi-coherent states*”, J.Phys. A: Math. Theor. 54 (2021) 055401; arXiv:2009.03400.
- [91] David Berenstein, Eric Dzienkowski, “*Matrix embeddings on flat \mathbb{R}^3 and the geometry of membranes*”, Phys. Rev. D 86 (2012) 086001; arXiv:1204.2788.
- [92] Joanna L. Karczmarek, Ken Huai-Che Yeh, “*Noncommutative spaces and matrix embeddings on flat \mathbb{R}^{2n+1}* ”, JHEP 11 (2015) 146; arXiv:1506.07188.
- [93] Mathias Hudoba de Badyn, Joanna L. Karczmarek, Philippe Sabella-Garnier, Ken Huai-Che Yeh, “*Emergent geometry of membranes*”, JHEP 11 (2015) 089; arXiv:1506.02035.
- [94] Kazuki Hasebe, in preparation.
- [95] Yusuke Kimura, “*Noncommutative gauge theory on fuzzy four-sphere and matrix model*”, Nucl.Phys.B 637 (2002) 177; hep-th/0204256.

- [96] Tsuguhiko Asakawa, Shigeki Sugimoto, Seiji Terashima, “*Exact Description of D-branes via Tachyon Condensation*”, JHEP 0302 (2003) 011; hep-th/0212188.
- [97] Seiji Terashima, “*Noncommutativity and Tachyon Condensation*”, JHEP 0510 (2005) 043; arXiv:hep-th/0505184.
- [98] Anton Kapustin and Lev Spodyneiko, “*Higher-dimensional generalizations of Berry curvature*”, Phys. Rev. B 101 (2020) 235130; arXiv:2001.03454.
- [99] A. Kitaev, “*Differential forms on the space of statistical mechanical lattice models*”, talk at Between Topology and Quantum Field Theory: a conference in celebration of Dan Freed’s 60th birthday, <https://web.ma.utexas.edu/topqft/talkslides/kitaev.pdf>.
- [100] Yusuke Kimura, “*Noncommutative Gauge Theories on Fuzzy Sphere and Fuzzy Torus from Matrix Model*”, Prog.Theor.Phys. 106 (2001) 445-469; hep-th/0103192.
- [101] Satoshi Iso, Yusuke Kimura, Kenji Tanaka, Kazunori Wakatsuki, “*Noncommutative gauge theory on fuzzy sphere from matrix model*”, Nucl. Phys. B 604 (2001) 121-147; hep-th/0101102.